Orbit design and TDI simulation for LISA, TAIJI and other LISA-like GW missions

Wei-Tou Ni 倪维斗

National Tsing Hua University

Refs: Gang Wang and WTN, Numerical simulation of time delay interferometry for new LISA, TAIJI and other LISA-like missions (2017)

WTN, GW detection in space IJMPD 25 (2016) 1530002

引力波谱分类 The Gravitation-Wave (GW) Spectrum Classification

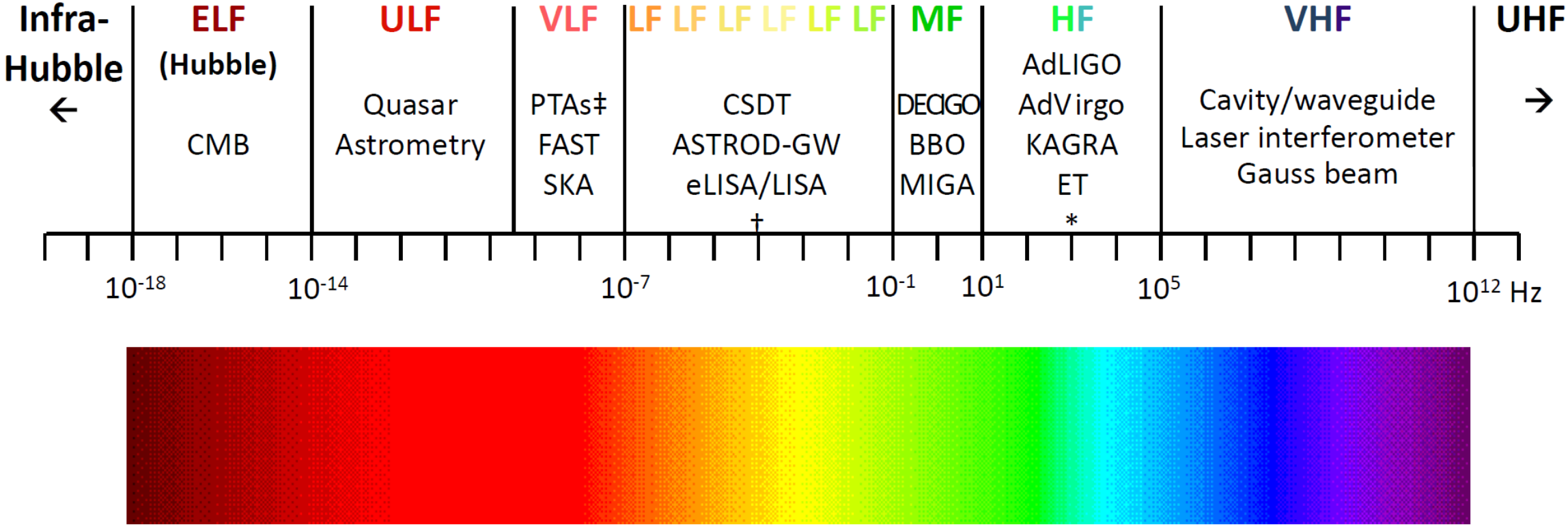

* AIGO, AURIGA, EXPLORER, GEO, NAUTILUS, MiniGRAIL, Schenberg.

† OMEGA, gLISA/GEOGRAWI, GADFLI, TIANQIN, ASTROD-EM, LAGRANGE, ALIA, ALIA-descope.

‡ EPTA, NANOGrav, PPTA, IPTA.

Scope: Goals –GW Astronomy & Fundamental Physics

Frequency band	GW sources / Possible GW sources	Detection method
Ultrahigh frequency band: above 1 THz	Discrete sources, Cosmological sources, Braneworld Kaluza-Klein (KK) mode radiation, Plasma instabilities	Terahertz resonators, optical resonators, and magnetic conversion detectors
Very high frequency band: 100 kHz – 1 THz	Discrete sources, Cosmological sources, Braneworld Kaluza-Klein (KK) mode radiation, Plasma instabilities	Microwave resonator/wave guide detectors, laser interferometers and Gaussian beam detectors
High frequency band (audio band)*: 10 Hz – 100 kHz	Conpact binaries [NS (Neutron Star)-NS, NS-BH (Black Hole), BH-BH], Supernovae	Low-temperature resonators and Earth-based laser-interferometric detectors
Middle frequency band: 0.1 Hz – 10 Hz	Intermediate mass black hole binaries, massive star (population III star) collapses	Space laser-interferometric detectors of arm length 1,000 km − 60,000 km
Low frequency band (milli-Hz band)†: 100 nHz – 0.1 Hz	Massive black hole binaries, Extreme mass ratio inspirals (EMRIs), Compact binaries	Space laser-interferometric detectors of arm length longer than 60,000 km
Very low frequency band (nano-Hz band): 300 pHz – 100 nHz	Supermassive black hole binary (SMBHB) coalescences, Stochastic GW background from SMBHB coalescences	Pulsar timing arrays (PTAs)
Ultralow frequency band: 10 fHz – 300 pHz	Inflationary/primordial GW background, Stochastic GW background	Astrometry of quasar proper motions
Extremely low (Hubble) frequency band: 1 aHz–10 fHz	Inflationary/primordial GW background	Cosmic microwave background experiments
Beyond Hubble-frequency band: below 1 aHz	Inflationary/primordial GW background	Through the verifications of primordial cosmological models

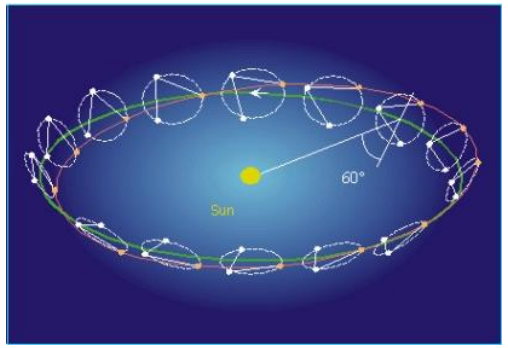

空间引力波探测
A Compilation of GW Mission Proposals LISA Pathfinder Launched on December 3, 2015

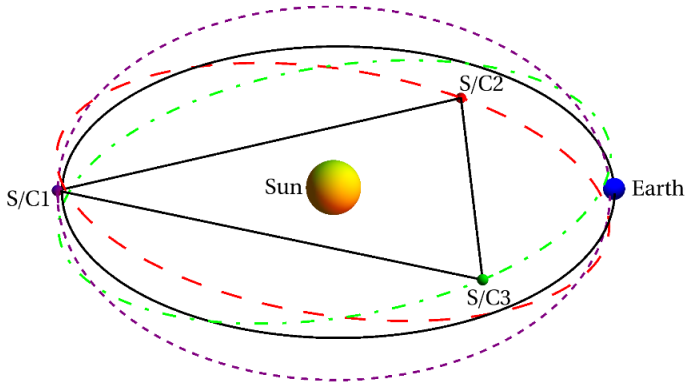

Mission Concept	S/C Configuration	Arm length	Orbit Period	S/C #
Solar-Orbit GW Mission Proposals				
LISA[65]	Earth-like solar orbits with 20° lag	5 Gm	1 year	3
eLISA[64]	Earth-like solar orbits with 10° lag	1 Gm	1 year	3
ASTROD-GW[68]	Near Sun-Earth L3, L4, L5 points	260 Gm	1 year	3
Big Bang Observer[73]	Earth-like solar orbits	0.05 Gm	1 year	12
DECIGO[72]	Earth-like solar orbits	0.001 Gm	1 year	12
ALIA[74]	Earth-like solar orbits	0.5 Gm	1 year	3
ALIA-descope[73]太极	Earth-like solar orbits	3 Gm	1 year	3
Super-ASTROD[71]	Near Sun-Jupiter L3, L4, L5 points (3 S/C), Jupiter-like solar orbit(s)(1-2 S/C)	1300 Gm	11 year	4 or 5
Earth-Orbit GW Mission Proposals				
OMEGA[81]	0.6 Gm height orbit	1 Gm	53.2 days	6
gLISA/GEOGRAWI[76-78]	Geostationary orbit	0.073 Gm	24 hours	3
GADFLI[79]	Geostationary orbit	0.073 Gm	24 hours	3
TIANQIN[82] 天琴	0.057 Gm height orbit	0.11 Gm	44 hours	3
ASTROD-EM[69,70]	Near Earth-Moon L3, L4, L5 points	0.66 Gm	27.3 days	3
LAGRANGE[80]	Near Earth-Moon L3, L4, L5 points	0.66 Gm	27.3 days	3

Science Goals

- The science goals are the detection of GWs from

- (i) Supermassive Black Holes;
- (ii) Extreme-Mass-Ratio Black Hole Inspirals;
- (iii) Intermediate-Mass Black Holes;
- (iv) Galactic Compact Binaries;
- (v) Relic/Inflationary GW Background.

Massive Black Hole Systems: Massive BH Mergers & Extreme Mass Ratio Mergers (EMRIs)

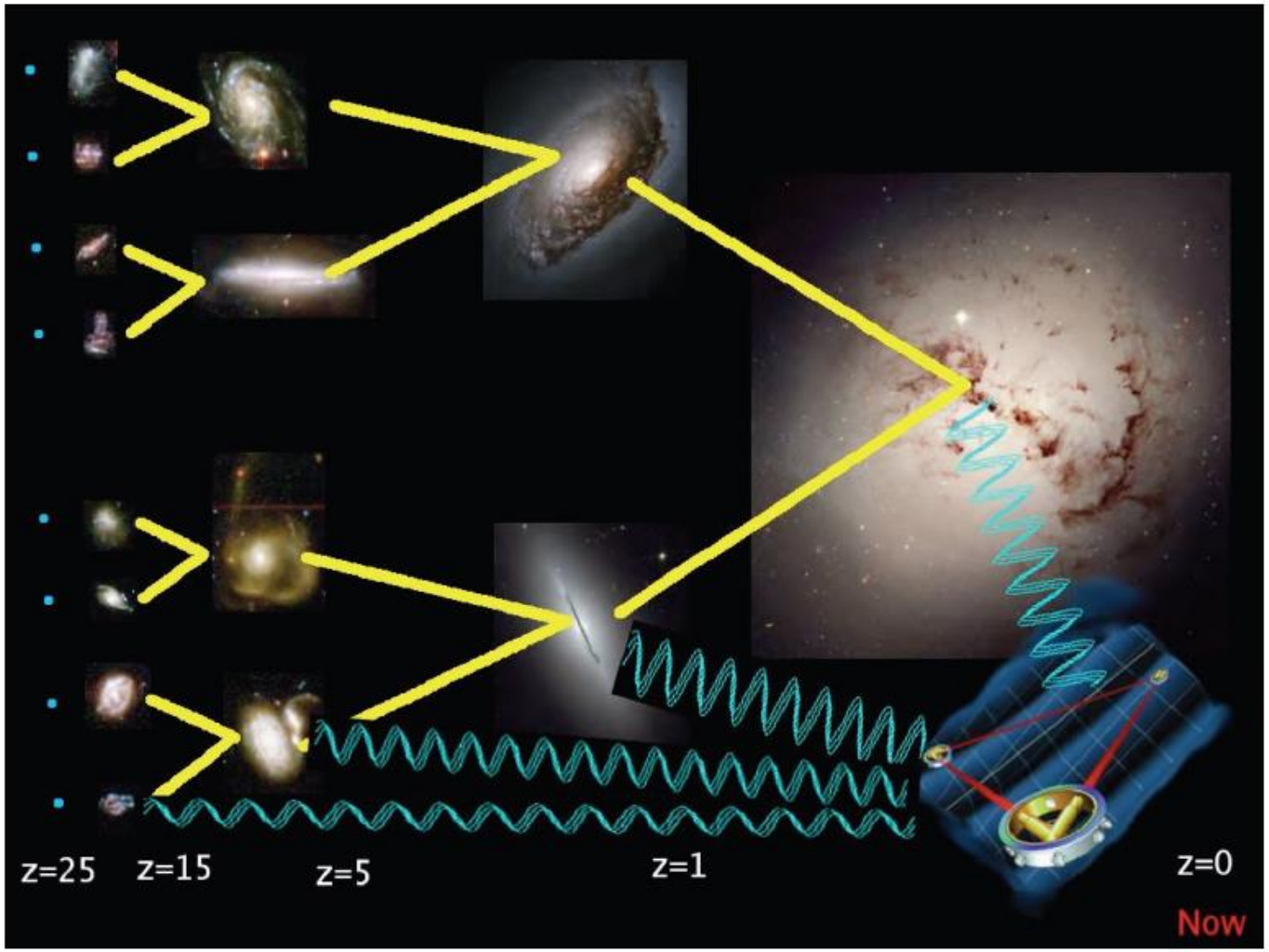

Outline

- INTRODUCTION – LISA-like Missions, Orbit configuration and TDI (time delay interferometry)
- Orbit Design
- Numerical TDI Calculation
- OUTLOOK

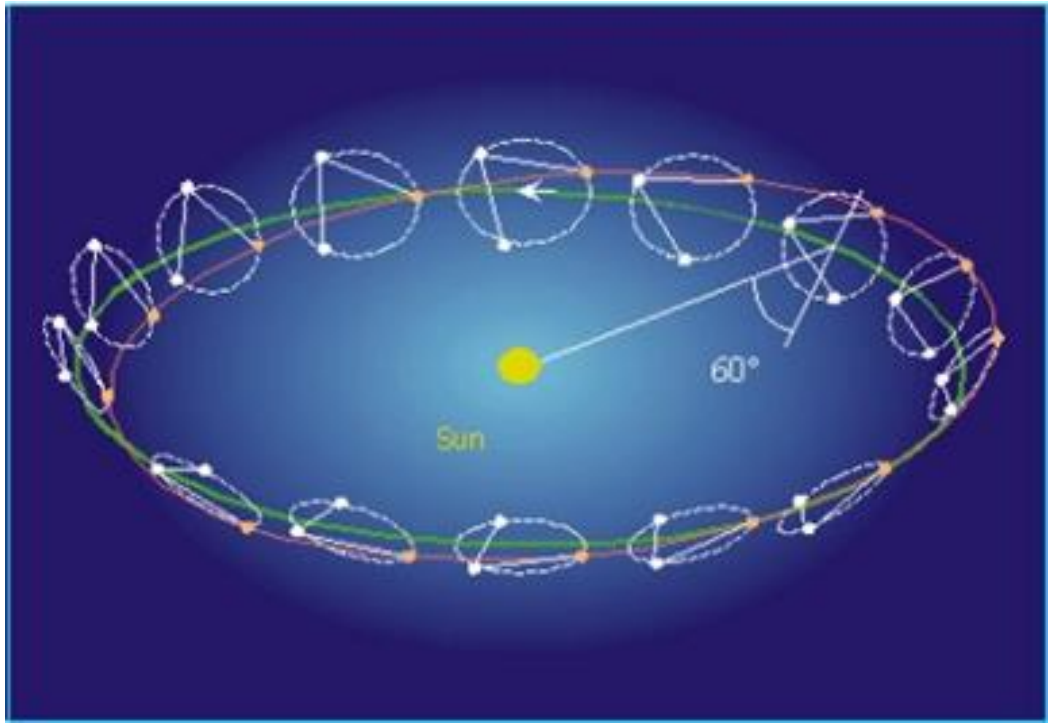

Hulse-Taylor Binary PSR1913+16

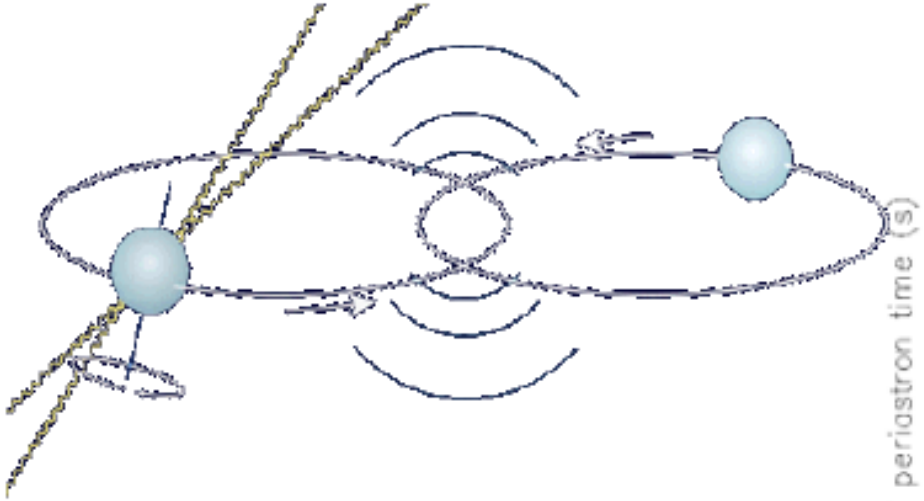

- Observed loss of energy matches prediction of GW emission to (0.13 ± 0.21)% **0.997±0.002(2010)**
- Indirect evidence of gravitational waves
- Frequency 70 μHz, amplitude 7×10^{-23} ⇒ outside detector sensitivity

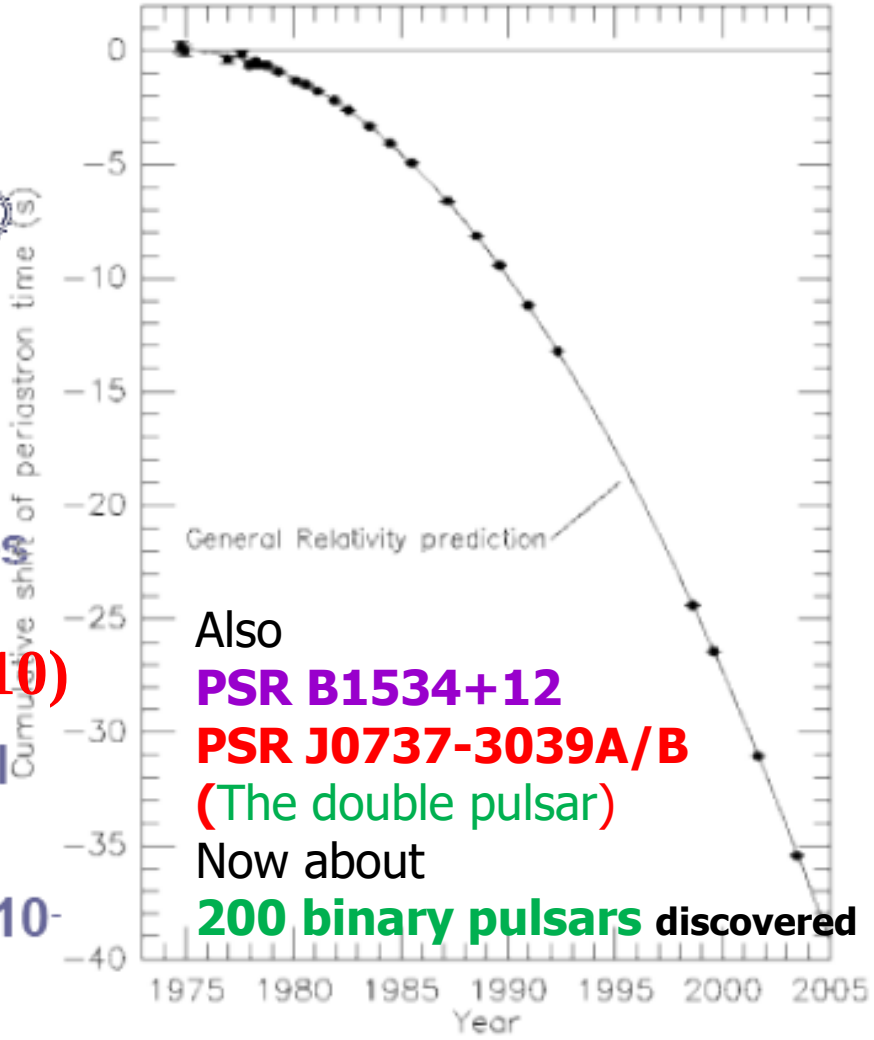

Also
PSR B1534+12
PSR J0737-3039A/B
(The double pulsar)
Now about
200 binary pulsars discovered

Gap largely bridged

92 days
1440 orbits
83.60 kg mass

- First artificial satellite Sputnik launched in 1957.
- First GW space mission proposed in public in 1981 by Faller & Bender
- LISA proposed as a joint ESA-NASA mission; LISA Pathfinder successfully performed. The drag-free tech is fully demonstrated paving the road for GW space missions.

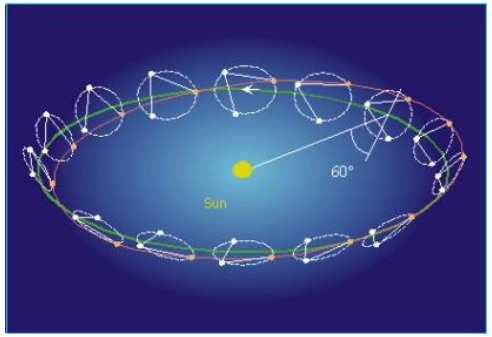

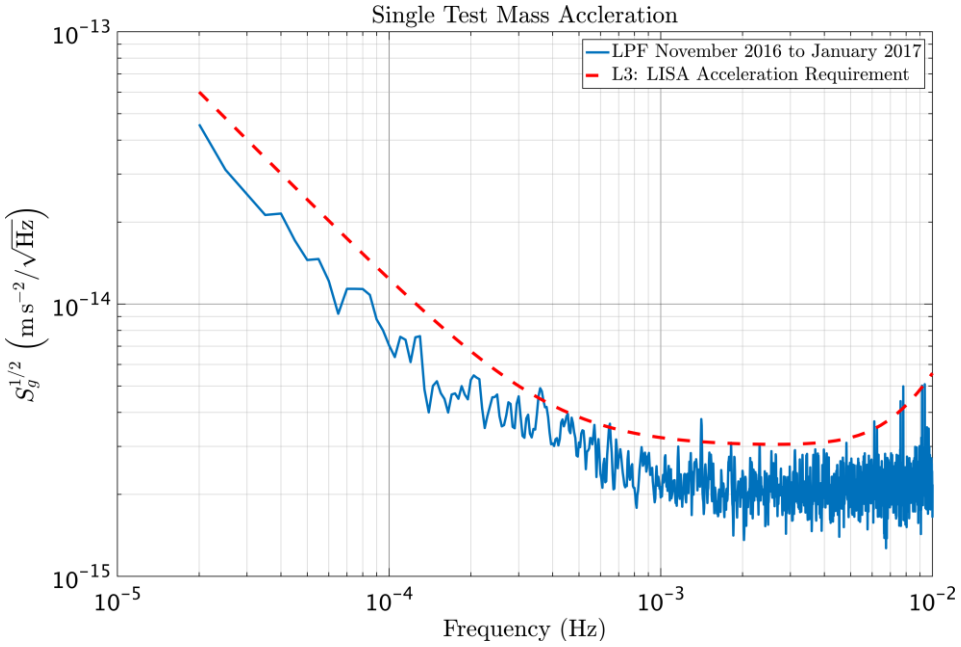

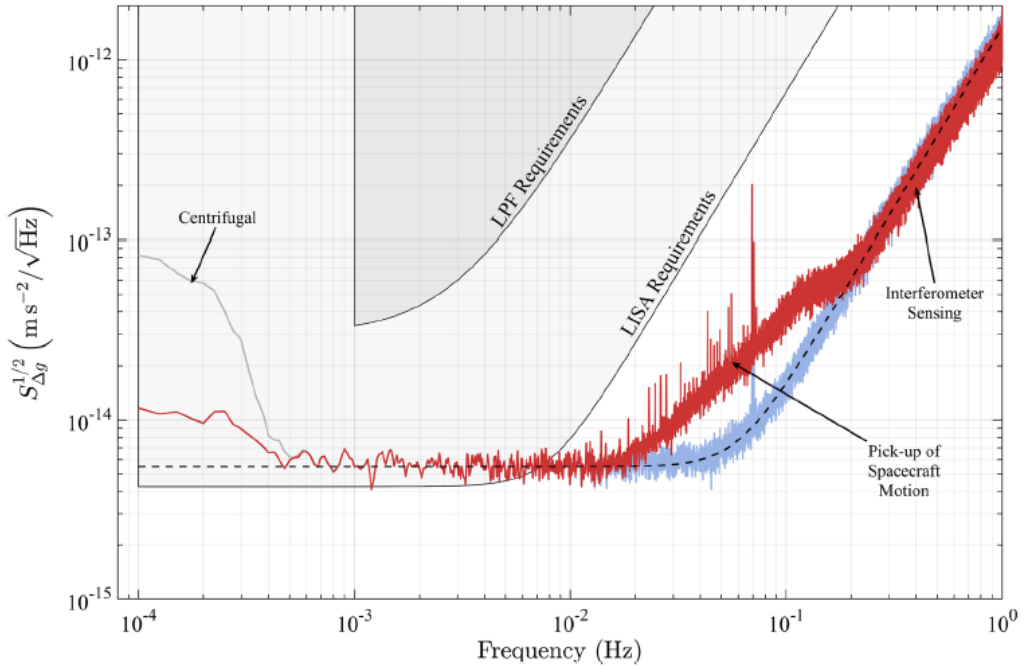

Weak-light phase locking and manipulation technology

- Weak-light phase locking is crucial for long-distance space interferometry and for CW laser space communication. For LISA of arm length of 5 Gm (million km) the weak-light phase locking requirement is for 70 pW laser light to phase-lock with an onboard laser oscillator. For ASTROD-GW arm length of 260 Gm (1.73 AU) the weak-light phase locking requirement is for 100 fW laser light to lock with an onboard laser oscillator. Weak-light phase locking for 2 pW laser light to 200 μW local oscillator is demonstrated in our laboratory in Tsing Hua U.[6] Dick *et al.*[7] from their phase-locking experiment showed a PLL (Phase Locked Loop) phase-slip rate below one cycle slip per second at powers as low as 40 femtowatts (fW).

The present laser stability (16 orders) alone does not meet the GW strain sensitivity requirement (21 orders)

- For space laser-interferometric GW antenna, the arm lengths vary according to solar system orbit dynamics.
- In order to attain the requisite sensitivity, laser frequency noise must be suppressed below the secondary noises such as the optical path noise, acceleration noise etc.
- For suppressing laser frequency noise, it is necessary to use TDI in the analysis to match the optical path length of different beam paths closely.
- The better match of the optical path lengths is, the better cancellation of the laser frequency noise and the easier to achieve the requisite sensitivity. In case of exact match, the laser frequency noise is fully canceled, as in the original Michelson interferometer.

Time Delay Interferometry (TDI)

first used in the study of ASTROD mission concept in the 1990s (Ni *et al*. 1997a, 1997b), two TDI configurations were used during the study of ASTROD interferometry and the path length differences were numerically obtained using Newtonian dynamics

- These two TDI configurations are the unequal arm Michelson TDI configuration and the Sagnac TDI configuration for three spacecraft formation flight. The principle is to have two split laser beams to go to Paths 1 and 2 and interfere at their end path. For unequal arm Michelson TDI configuration, one laser beam starts from spacecraft 1 (S/C1) directed to and received by spacecraft 2 (S/C2), and optical phase locking the local laser in S/C2; the phase locked laser beam is then directed to and received by S/C1, and optical phase locking another local laser in S/C1; and so on to return to S/C1:
- Path 1: S/C1 → S/C2 → S/C1 → S/C3 → S/C1. (1)
- The second laser beam starts from S/C1 also:
- Path 2: S/C1 → S/C3 → S/C1 → S/C2 → S/C1, (2)
- to return to S/C1 and to interfere with the first beam.
- If the two paths has exactly the same optical path length,
- the laser frequency noises cancel out; if the optical path length difference is small, the laser frequency noises cancel to a large extent. In the Sagnac TDI configuration, the two paths are:
- Path 1: S/C1 → S/C2 → S/C3 → S/C1, Path 2: S/C1 → S/C3 → S/C2 → S/C1.

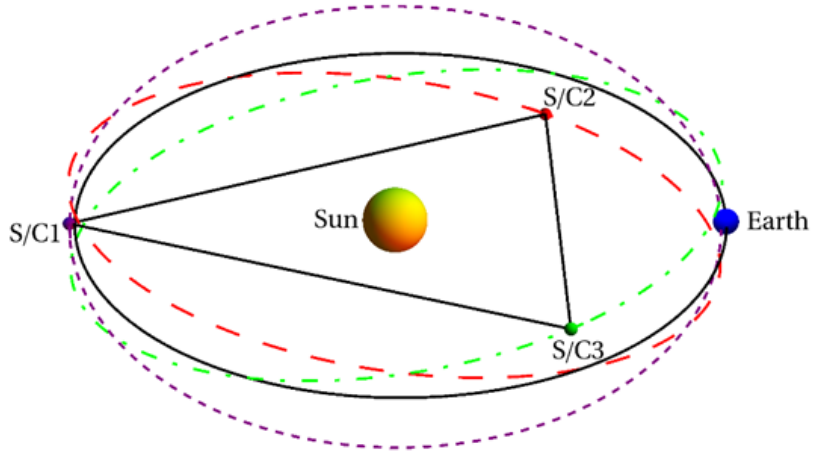

Unequal-arm Michelson X, Y & Z TDIs and its sum X+Y+Z for new LISA

- 1999 Armstrong, Estabrook, Tinto, X, Y & Z TDIs X+Y+Z for LISA
- Vallisneri 2005 (U, P, E)
- Tinto & Dhurandhar review 2014

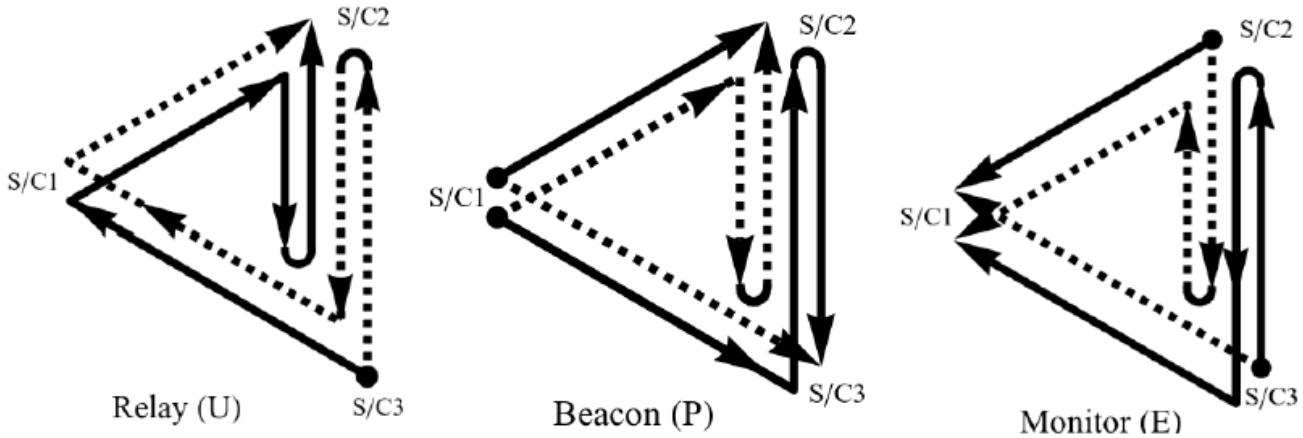

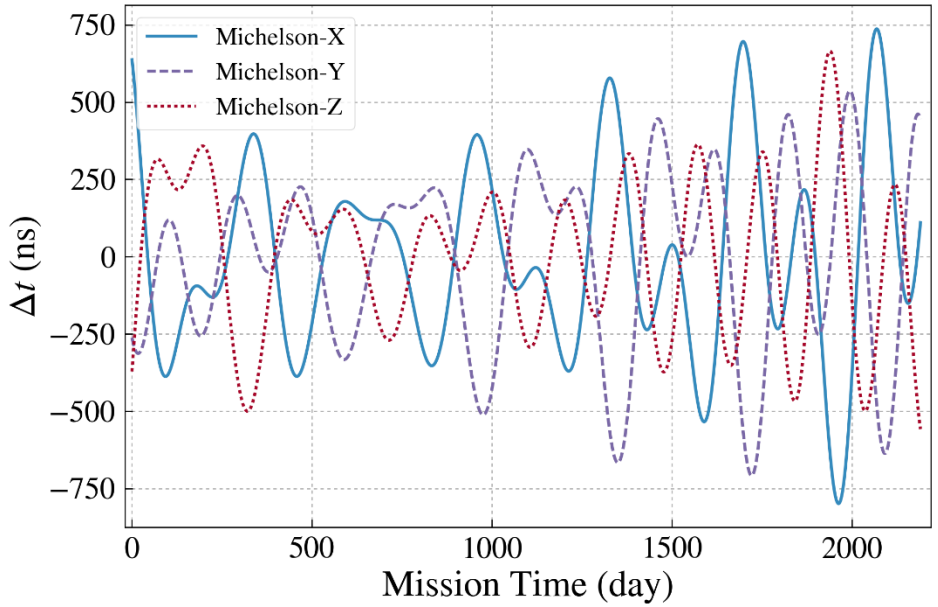

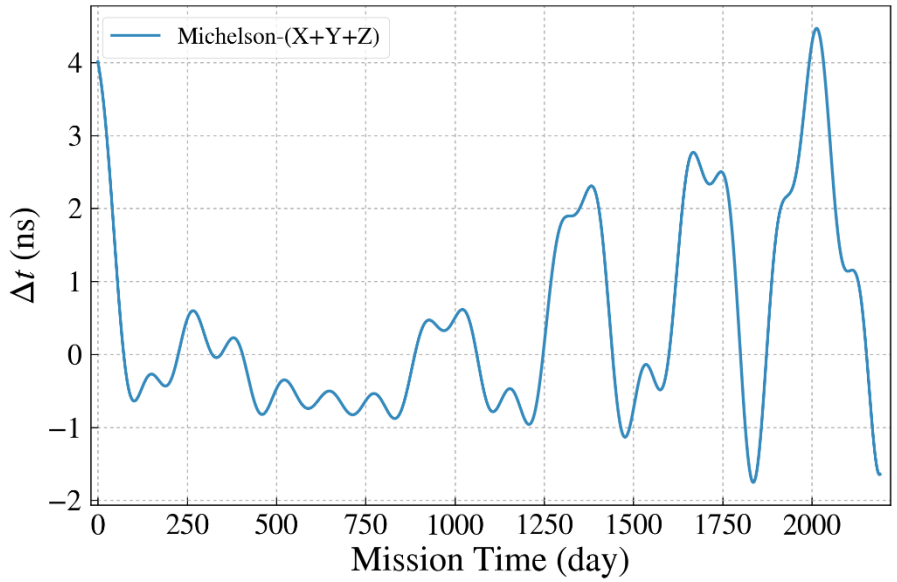

Orbit Design I – the initial choice of initial conditions

- Define X_{fk}, Y_{fk}, Z_{fk}, (k = 1.2, 3) to be

$$X_{fk} = R\,(\cos\psi_k + e)\cos\varepsilon\,,$$
$$Y_{fk} = R\,(1-e^2)^{1/2}\sin\psi_k\,,$$
$$Z_{fk} = R\,(\cos\psi_k + e)\sin\varepsilon.$$

$$\psi_k + e\sin\psi_k = \Omega\,(t-t_0) - 120°(k-1),\ \text{for } k = 1, 2, 3.$$

the eccentric anomaly

- Define $X_{f(k)}$, $Y_{f(k)}$, $Z_{f(k)}$, (k = 1.2, 3), i.e., $X_{f(1)}$, $Y_{f(1)}$, $Z_{f(1)}$; $X_{f(2)}$, $Y_{f(2)}$, $Z_{f(2)}$; $X_{f(3)}$, $Y_{f(3)}$, $Z_{f(3)}$ to be

$$X_{f(k)} = X_{fk}\cos[120°(k-1)+\varphi_0] - Y_{fk}\sin[120°(k-1)+\varphi_0],$$
$$Y_{f(k)} = X_{fk}\sin[120°(k-1)+\varphi_0] + Y_{fk}\cos[120°(k-1)+\varphi_0],$$
$$Z_{f(k)} = Z_{fk}.$$

- The three S/C orbits are (for one-body central problem) are

$$\mathbf{R}_{S/C1} = (X_{f(1)}, Y_{f(1)}, Z_{f(1)}),$$
$$\mathbf{R}_{S/C2} = (X_{f(2)}, Y_{f(2)}, Z_{f(2)}),$$
$$\mathbf{R}_{S/C3} = (X_{f(3)}, Y_{f(3)}, Z_{f(3)}).$$

Using ephemeris framework for design and TDI numerical calculation

$$ds^2 = [1 - 2\sum_i \frac{m_i}{r_i} + 2\beta(\sum_i \frac{m_i}{r_i})^2 + (4\beta - 2)\sum_i \frac{m_i}{r_i}\sum_{j\neq i}\frac{m_j}{r_{ij}}$$

$$- c^{-2}\sum_i \frac{m_i}{r_i}(2(\gamma+1)\dot{\boldsymbol{x}}_i^2 - \boldsymbol{r}_i\cdot\ddot{\boldsymbol{x}}_i - \frac{1}{r_i^2}(\boldsymbol{r}_i\cdot\dot{\boldsymbol{x}}_i)^2) + \frac{m_1 R_1^2}{r_1^3}J_2(3(\frac{\boldsymbol{r}_1\cdot\hat{\boldsymbol{z}}}{r_1})^2 - 1)]c^2dt^2$$

$$+ 2c^{-1}\sum_i \frac{m_i}{r_i}((2\gamma+2)\dot{\boldsymbol{x}}_i)\cdot d\boldsymbol{x}cdt - [1 + 2\gamma\sum_i \frac{m_i}{r_i}](d\boldsymbol{x})^2 \qquad (40)$$

$$\ddot{\boldsymbol{x}}_i = -\sum_{j\neq i}\frac{GM_j}{r_{ij}^3}\boldsymbol{r}_{ij} + \sum_{j\neq i} m_j(A_{ij}\boldsymbol{r}_{ij} + B_{ij}\dot{\boldsymbol{r}}_{ij}),$$

$$A_{ij} = \frac{\dot{\boldsymbol{x}}_i^2}{r_{ij}^3} - (\gamma+1)\frac{\dot{\boldsymbol{r}}_{ij}^2}{r_{ij}^3} + \frac{3}{2r_{ij}^5}(\boldsymbol{r}_{ij}\dot{\boldsymbol{x}}_j)^2 + G[(2\gamma+2\beta+1)M_i + (2\gamma+2\beta)M_j]\frac{1}{r_{ij}^4}$$

$$+ \sum_{k\neq i,j} GM_k[(2\gamma+2\beta)\frac{1}{r_{ij}^3 r_{ik}} + (2\beta-1)\frac{1}{r_{ij}^3 r_{jk}} + \frac{2(\gamma+1)}{r_{ij}r_{jk}^3} - (2\gamma+\frac{3}{2})\frac{1}{r_{ik}r_{jk}^3} - \frac{1}{2r_{jk}^3}\frac{\boldsymbol{r}_{ij}\boldsymbol{r}_{ik}}{r_{ij}^3}],$$

$$B_{ij} = \frac{1}{r_{ij}^3}[(2\gamma+2)(\boldsymbol{r}_{ij}\dot{\boldsymbol{r}}_{ij}) + (\boldsymbol{r}_{ij}\dot{\boldsymbol{x}}_j)].$$

3 complete ephemeris + 1 ephemeris framework

- DE: Development Ephemerides
- EPM: Ephemerides of Planets and Moon
- INPOP: Intégrateur Numérique Planétaire de l'Observatoire de Paris
- CGC: Center for Gravitation and Cosmology Ephemeris Framework

Orbit design for New LISA (arm length 2.5 Gm) initial epoch: 2028-Mar-22nd 12:00:00 for 2200 days

		Initial choice of S/C initial states		Initial states of S/C after final optimization
S/C1 Position (AU)	X Y Z	-9.342358697598E-01 3.222028021891E-01 1.415510901823E-01	adjust to ==>	-9.342355891858E-01 3.222027047288E-01 1.415510473840E-01
S/C1 Velocity (AU/day)	V_x V_y V_z	-6.020533666442E-03 -1.471303796371E-02 -6.532104563056E-03	=	-6.020533666442E-03 -1.471303796371E-02 -6.532104563056E-03
S/C2 Position (AU)	X Y Z	-9.422917194822E-01 3.075956329521E-01 1.403200701890E-01	=	-9.422917194822E-01 3.075956329521E-01 1.403200701890E-01
S/C2 Velocity (AU/day)	V_x V_y V_z	-5.875601408922E-03 -1.480936170059E-02 -6.319195852807E-03	=	-5.875601408922E-03 -1.480936170059E-02 -6.319195852807E-03
S/C3 Position (AU)	X Y Z	-9.335382669969E-01 3.132742531958E-01 1.273476800288E-01	=	-9.335382669969E-01 3.132742531958E-01 1.273476800288E-01
S/C3 Velocity (AU/day)	V_x V_y V_z	-5.949351791423E-03 -1.490443611747E-02 -6.410590762560E-03	=	-5.949351791423E-03 -1.490443611747E-02 -6.410590762560E-03

Variations of the arm lengths and the velocities in the line of sight direction in 2200 days for the LISA S/C configuration with initial condition adjustment

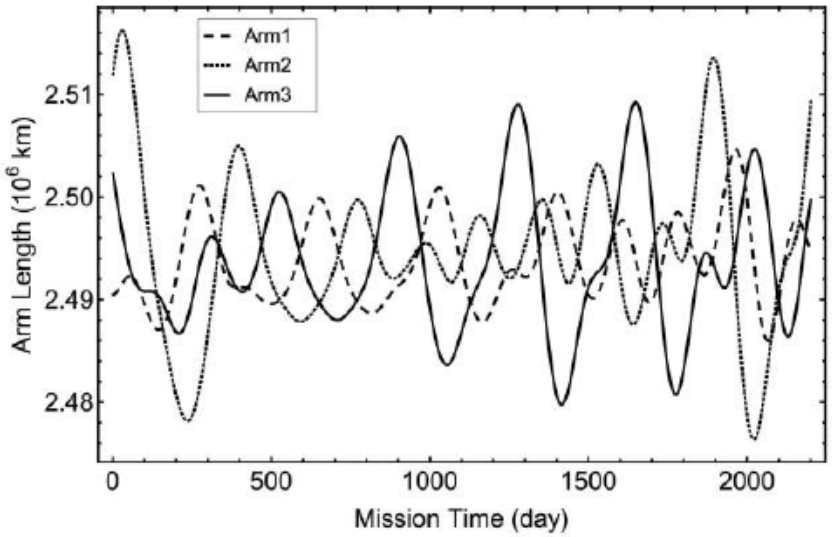

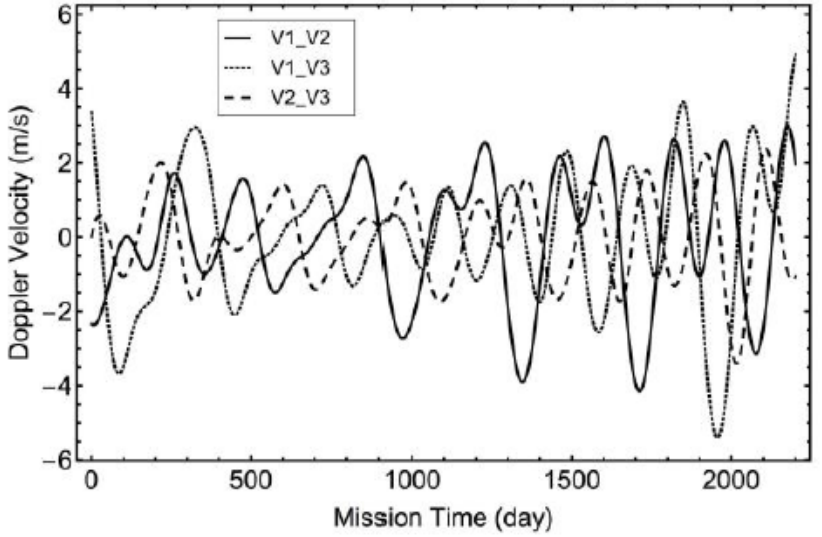

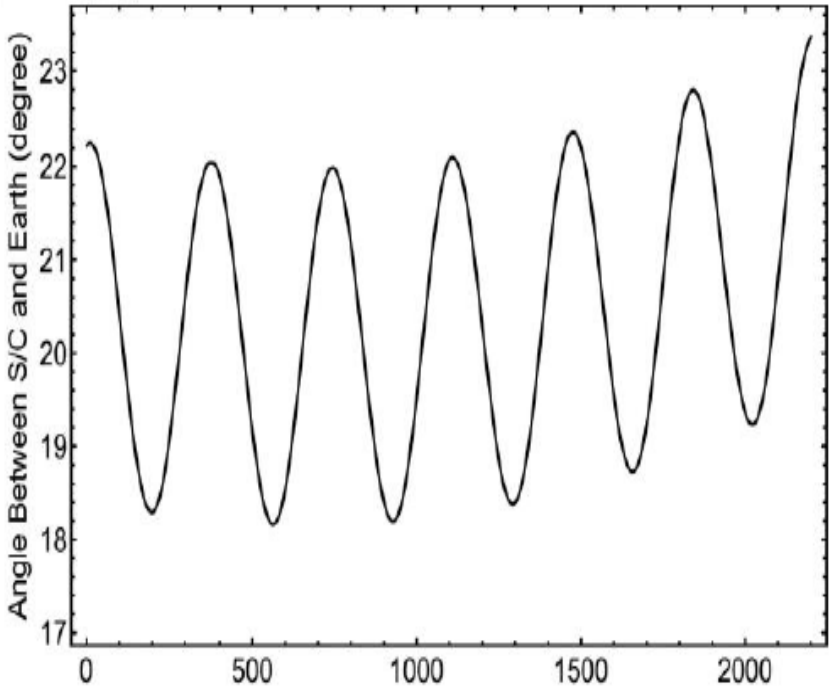

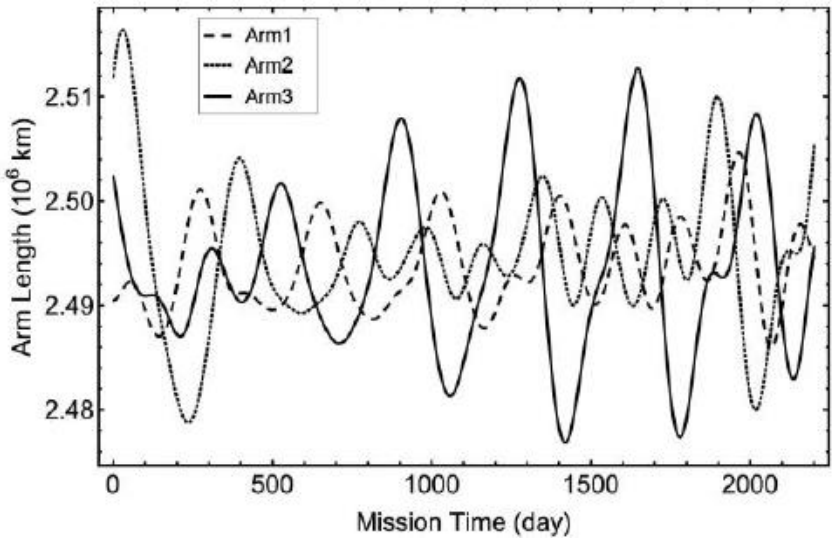

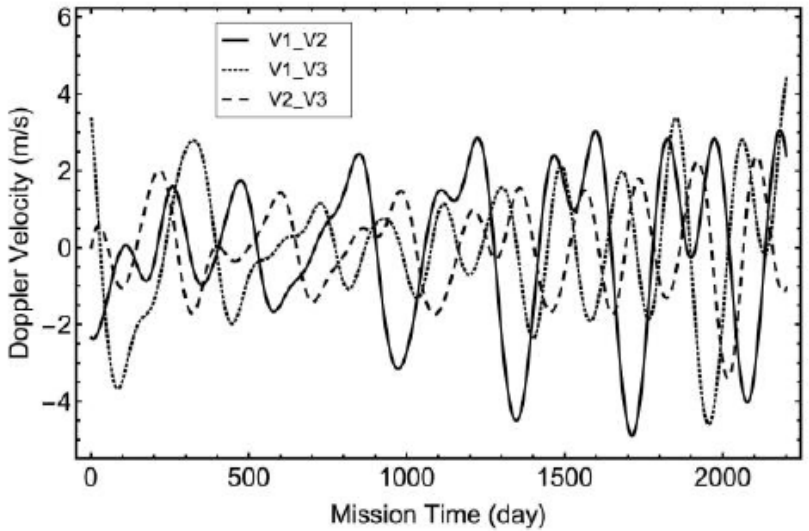

Variations of the arm lengths and the velocities in the line of sight direction in 2200 days for the TAIJI S/C configuration with initial condition adjustment

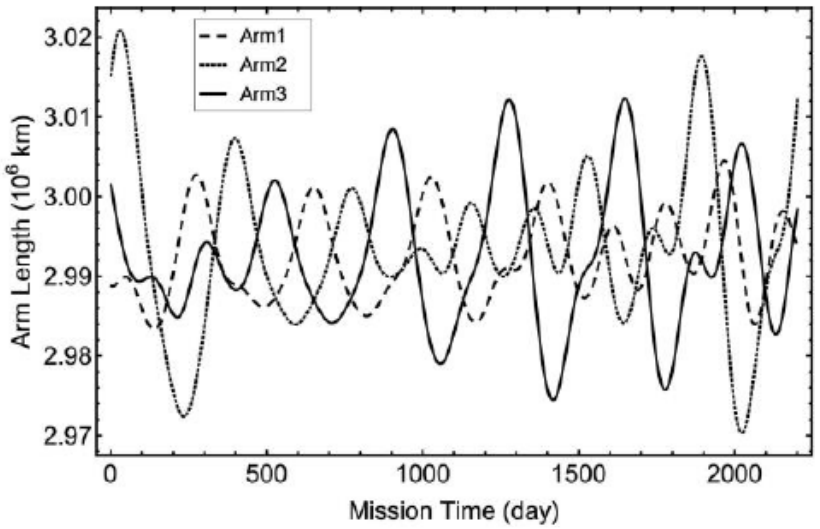

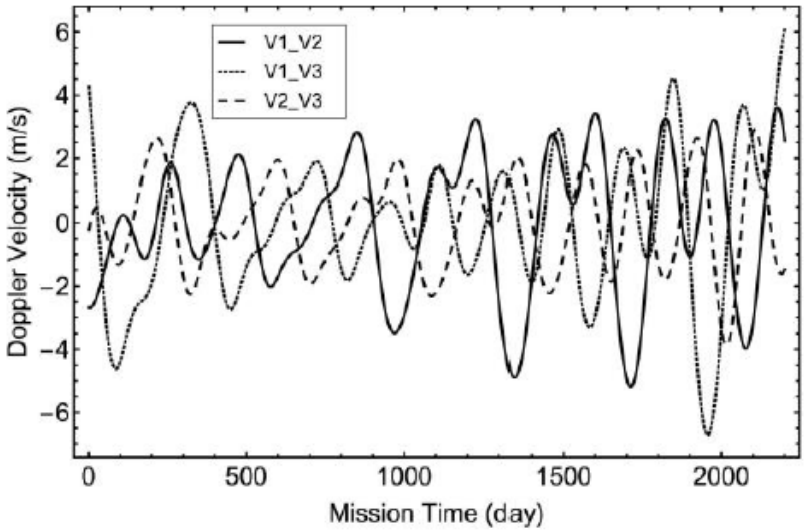

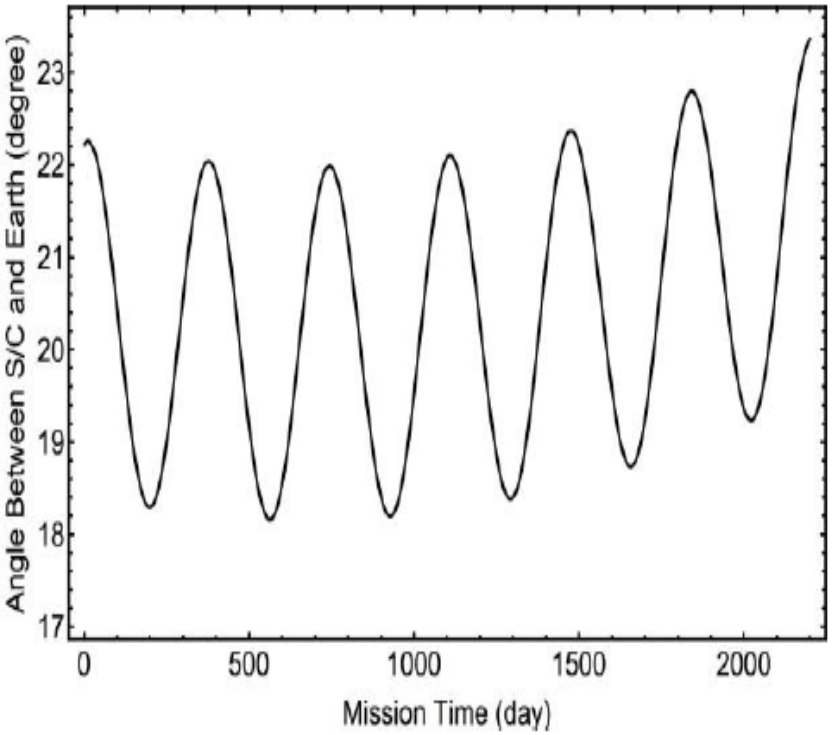

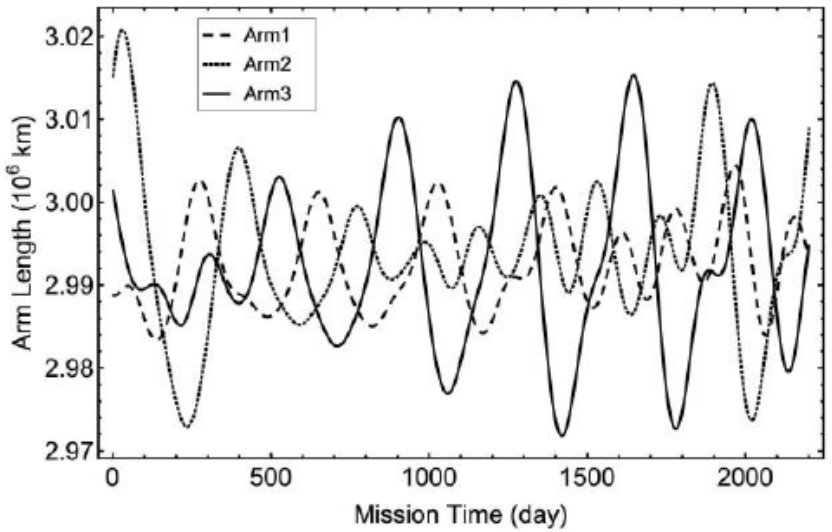

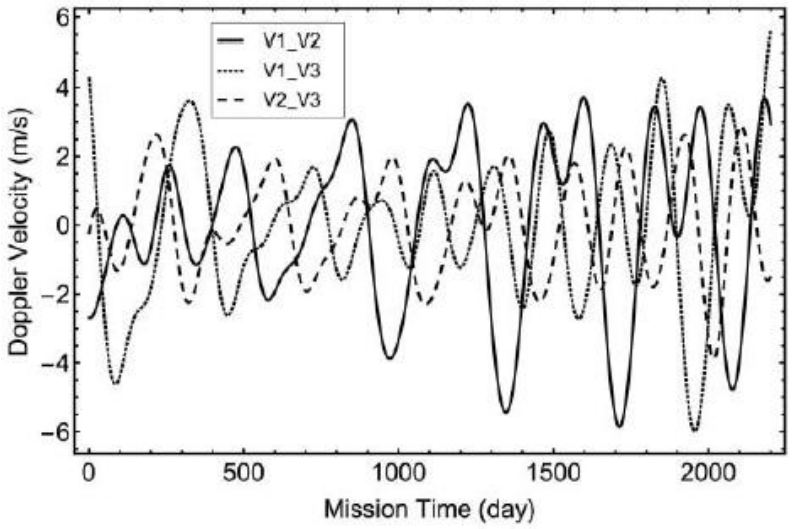

Unequal-arm Michelson X, Y & Z TDIs and its sum X+Y+Z for TAIJI

- 1999 Armstrong, Estabrook, Tinto, X, Y & Z TDIs X+Y+Z for LISA
- Vallisneri 2005 (U, P, E)
- Tinto & Dhurandhar review 2014

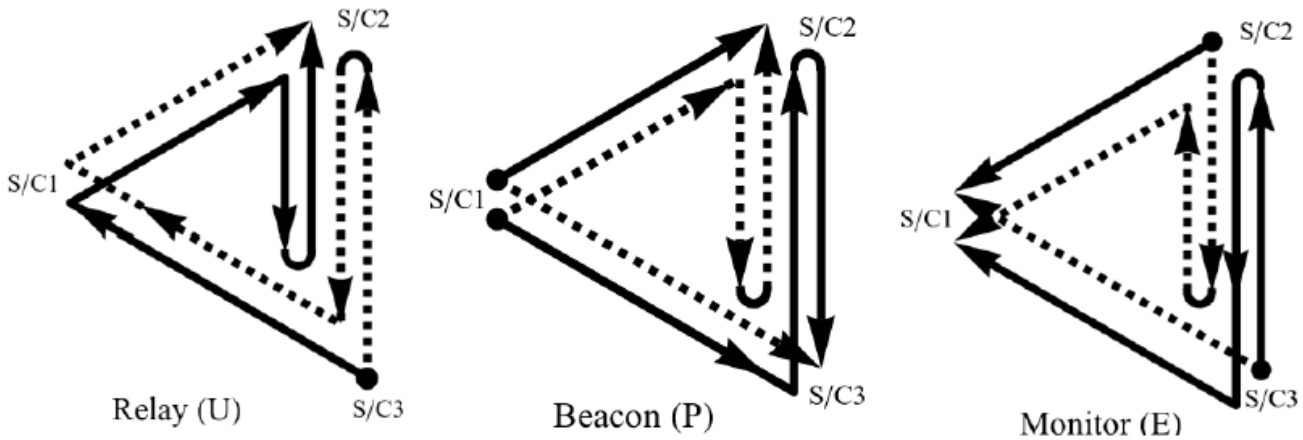

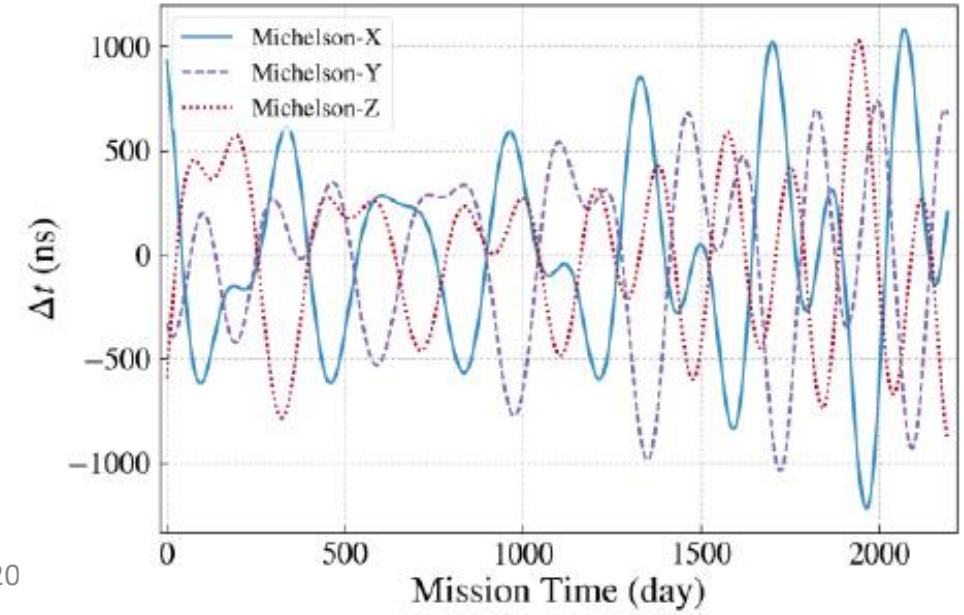

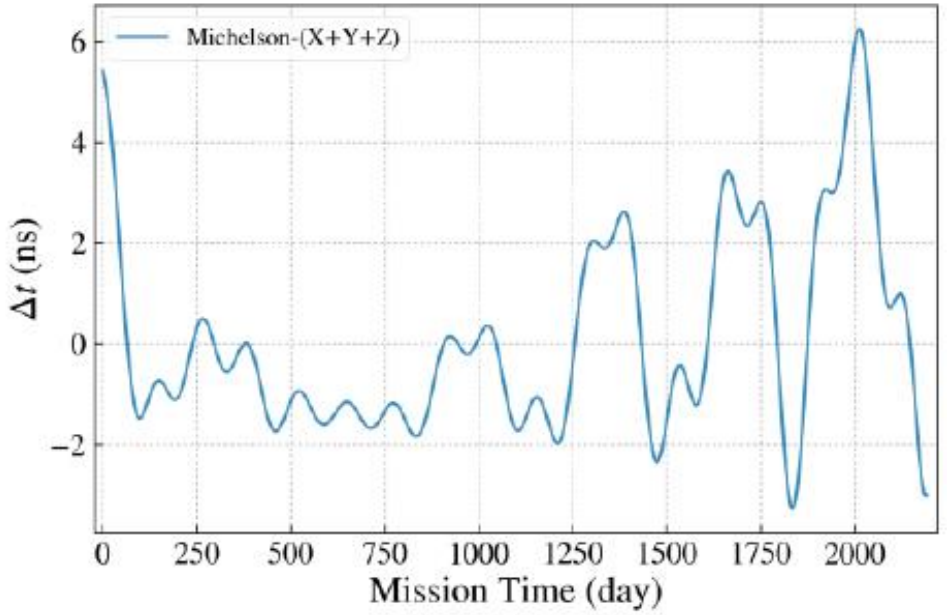

20

Sagnac α, β & γ; Relay U, V & W; Beacon P, Q & R; Monitor E, F & G first-generation TDIs of New LISA

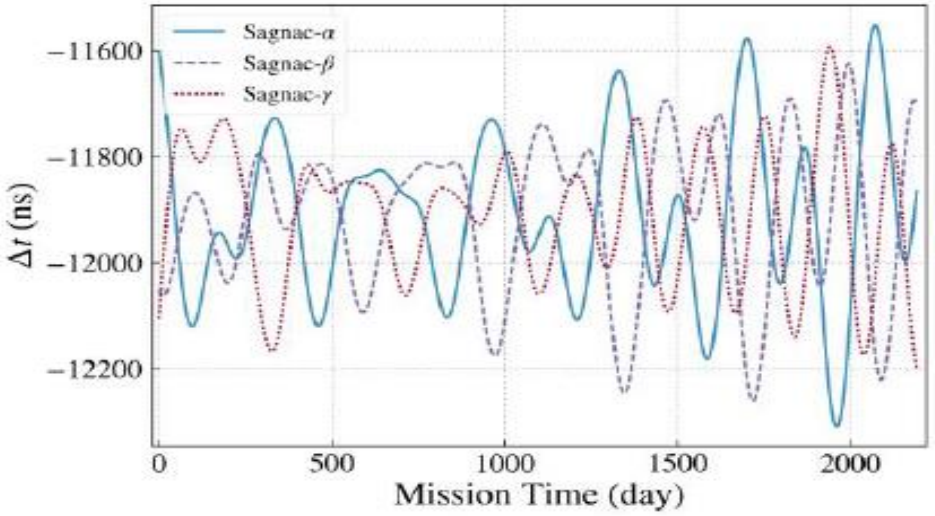

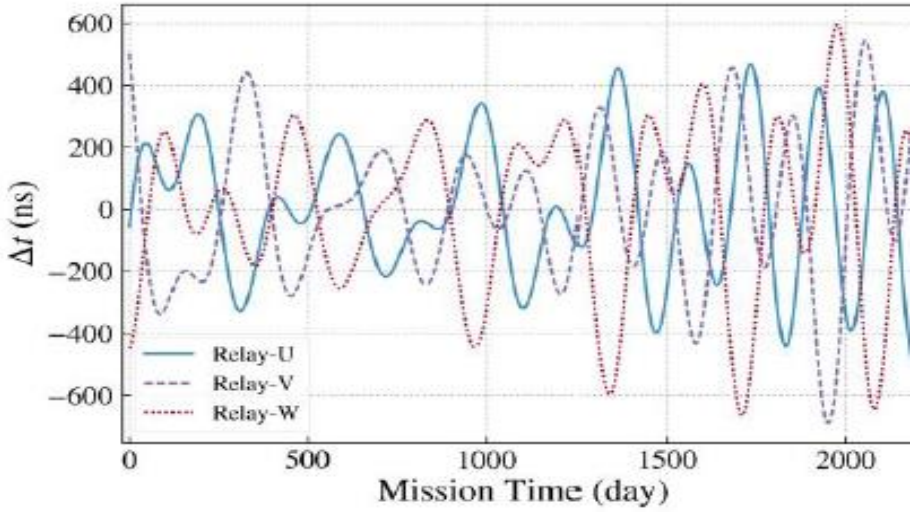

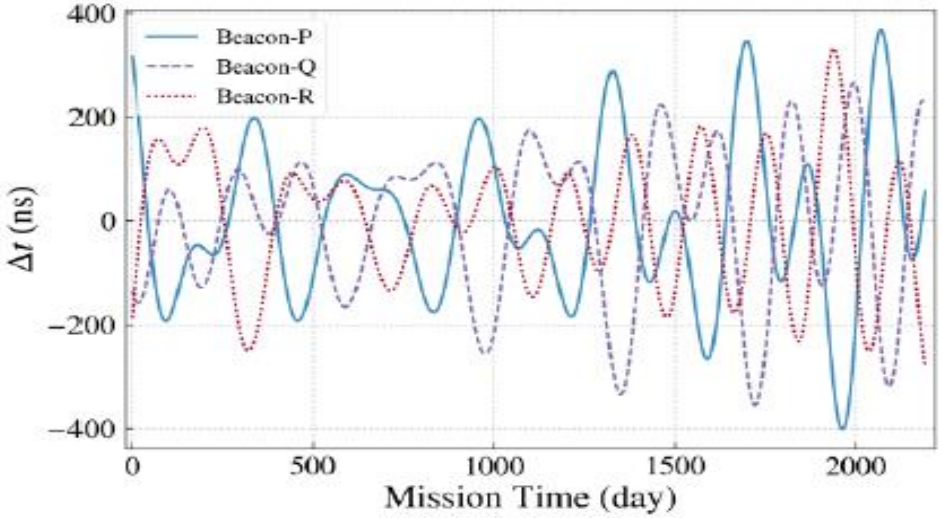

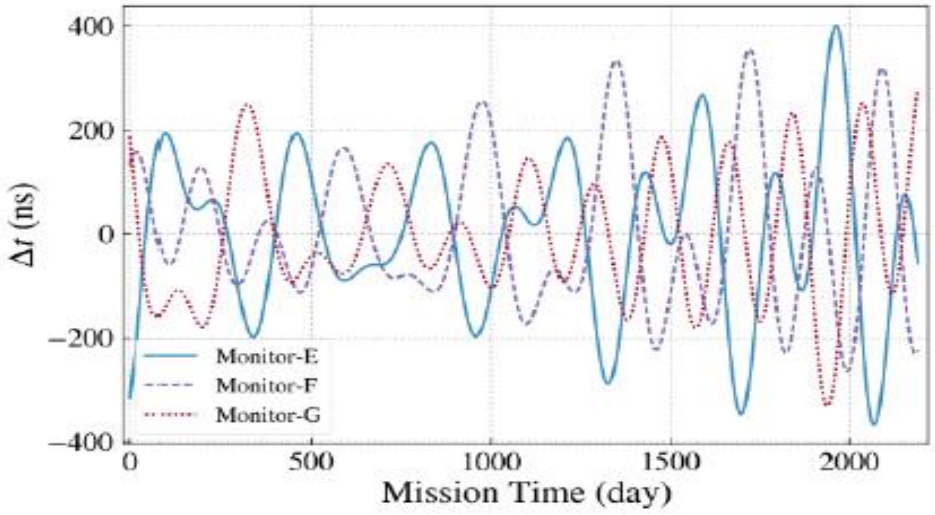

Sagnac α, β & γ; Relay U, V & W; Beacon P, Q & R; Monitor E, F & G first-generation TDIs of TAIJI

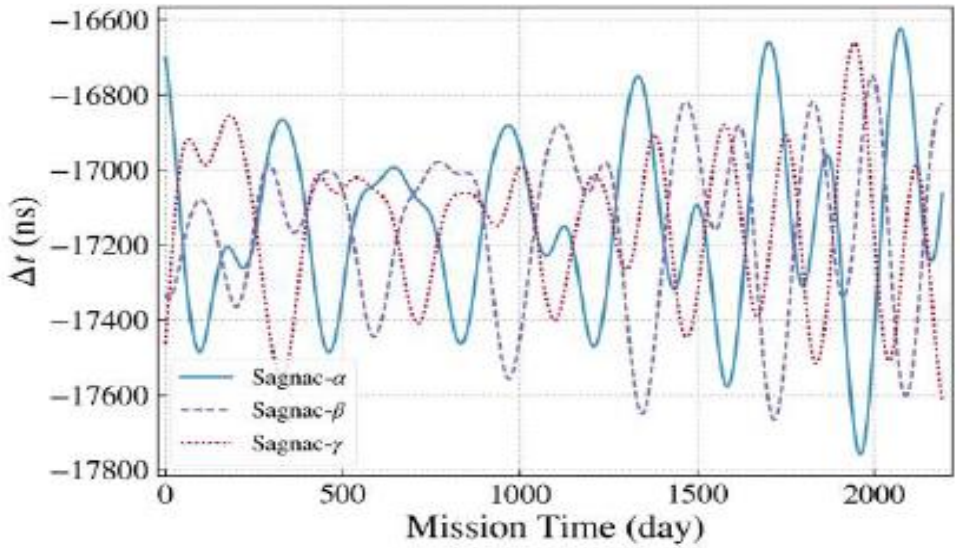

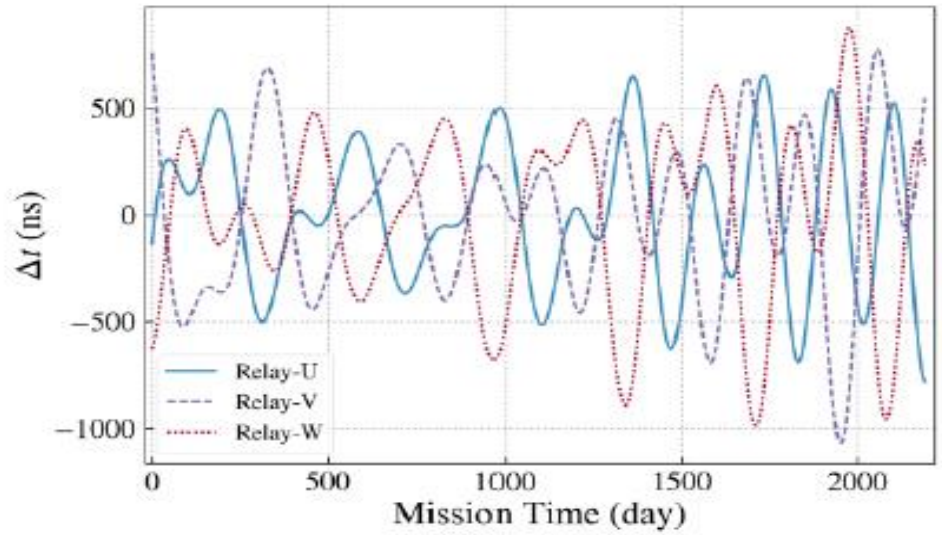

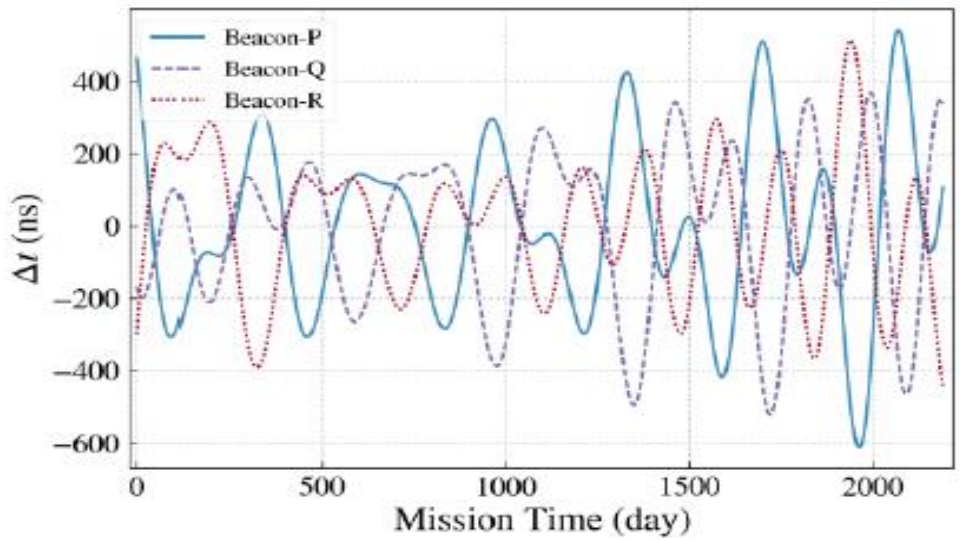

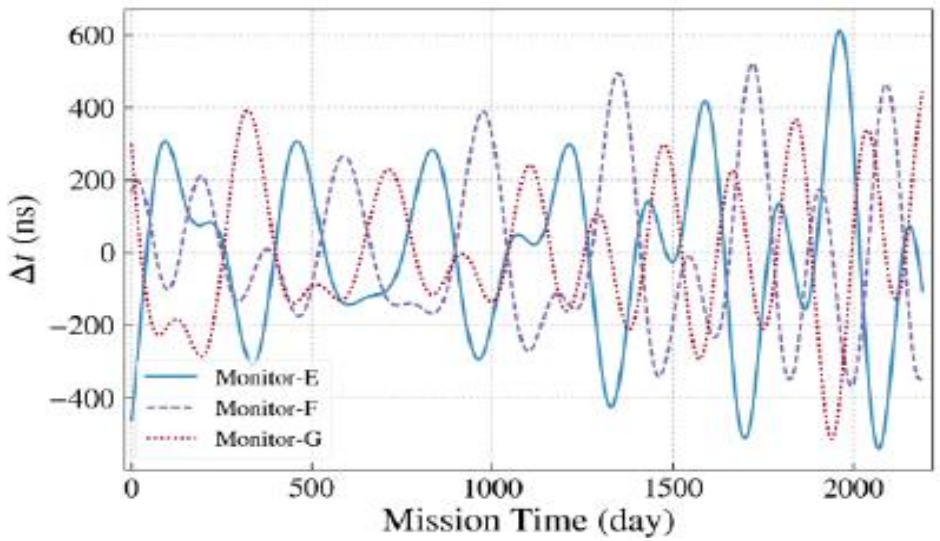

A comparison of cases for different arm lengths

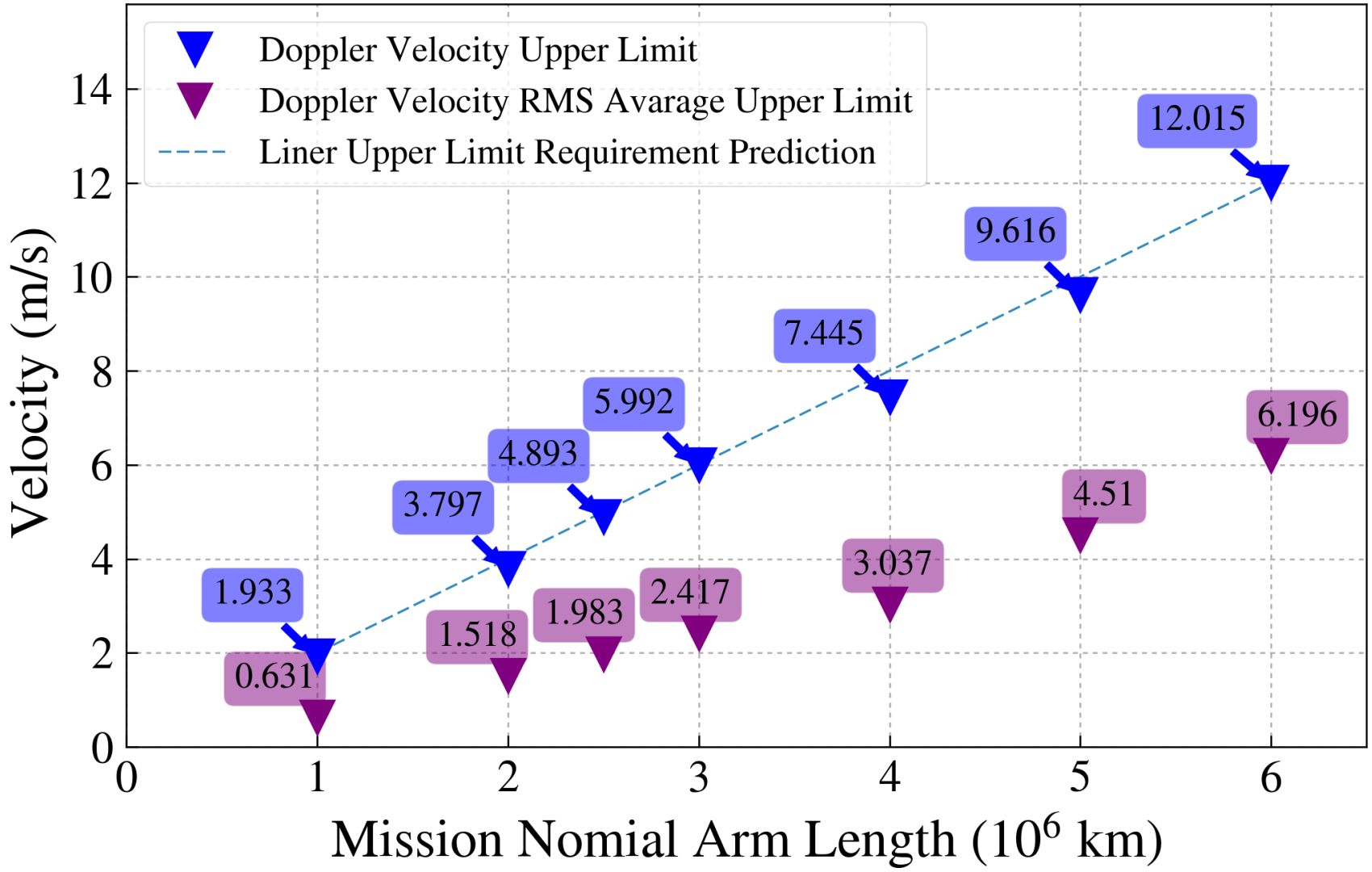

(X, Y, Z)TDI time-delay difference vs. epoch

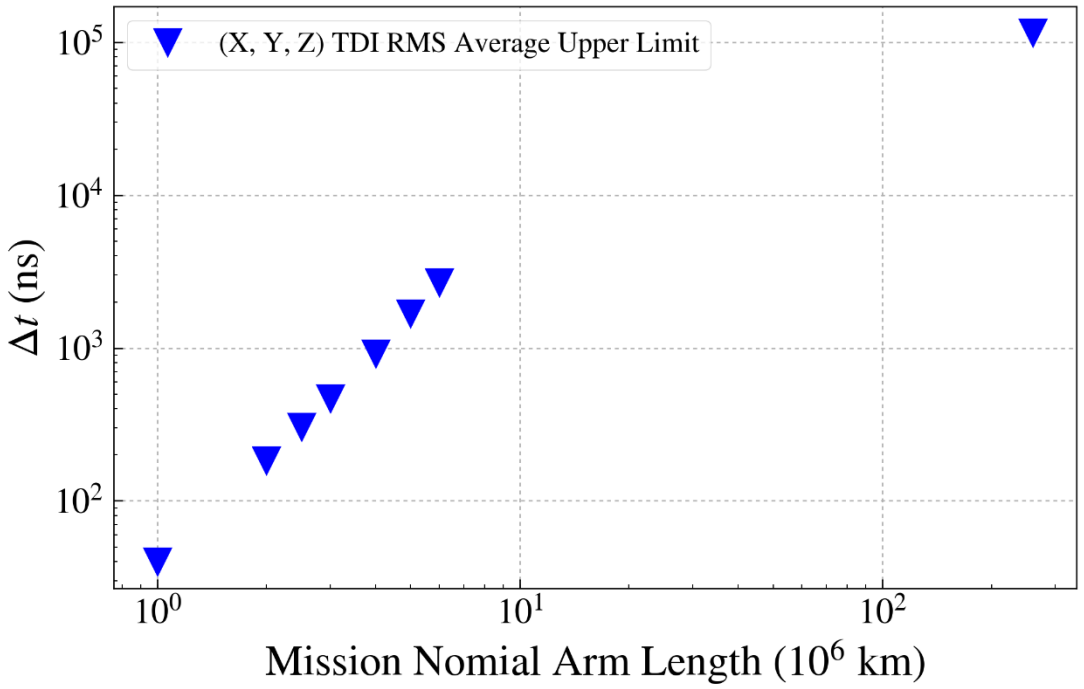

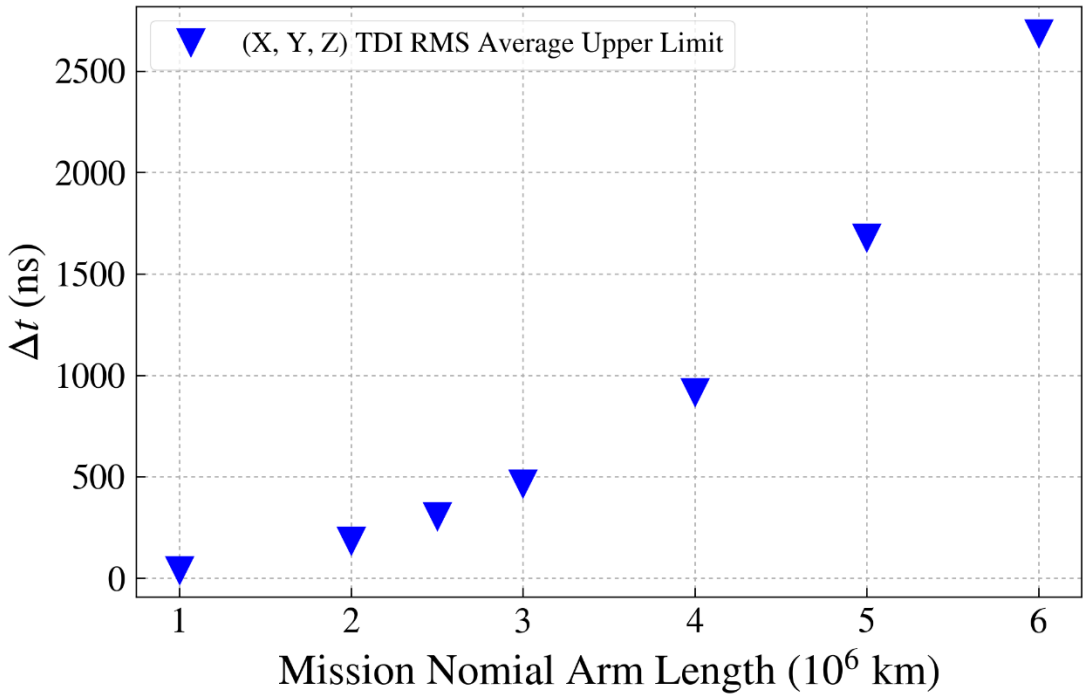

Discussion and Outlook

- All the first-generation TDIs violate their respective requirements. For eLISA/NGO of arm length 1 Gm, the deviation for X, Y, and Z TDIs could be up to a factor of 3.6; for the case of 2 Gm arm length, a factor of 6.8; for the new LISA case of 2.5 Gm arm length, a factor of 9.6; for the TAIJI case of 3 Gm arm length, a factor of 12.5; for the case of 4 Gm arm length, a factor of 15.2; for the original LISA of 5 Gm, a factor of 22.3; for the case of 6 Gm arm length, a factor 29.9. If X, Y, and Z TDIs are used for the GW analysis, either the TDI requirement needs to be relaxed by the same factor or laser frequency stability requirement needs to be strengthened by the same factor.
- All the second-generation TDIs in Table 2 for eLISA/NGO of arm length 1 Gm, for the case of 2 Gm arm length and for the new LISA case of 2.5 Gm arm length satisfy their respective requirements.

Strain power spectral density (psd) amplitude vs. frequency for various GW detectors and GW sources. [CSDT: Cassini Spacecraft Doppler Tracking; SMBH-GWB: Supermassive Black Hole-GW Background.]

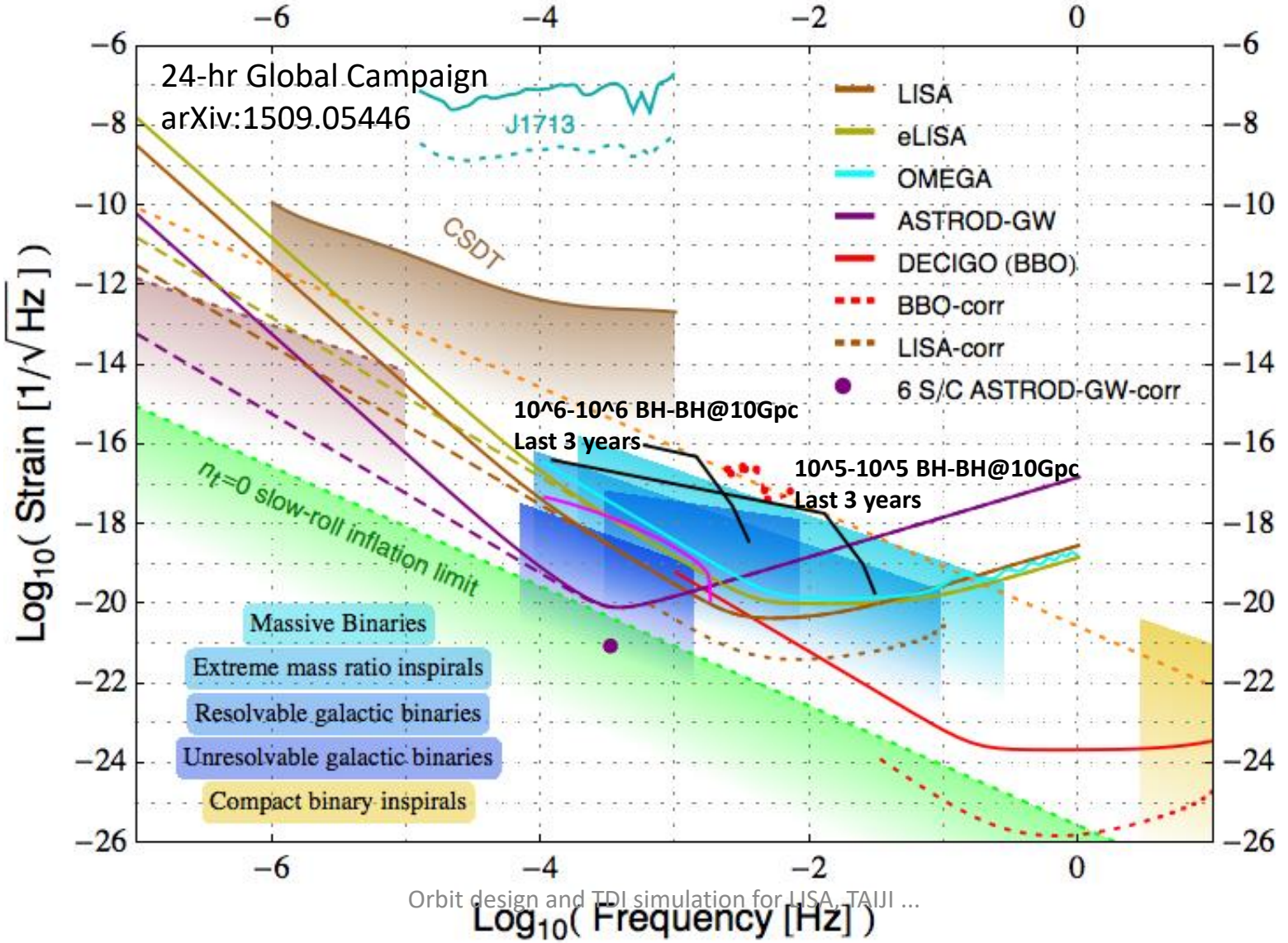

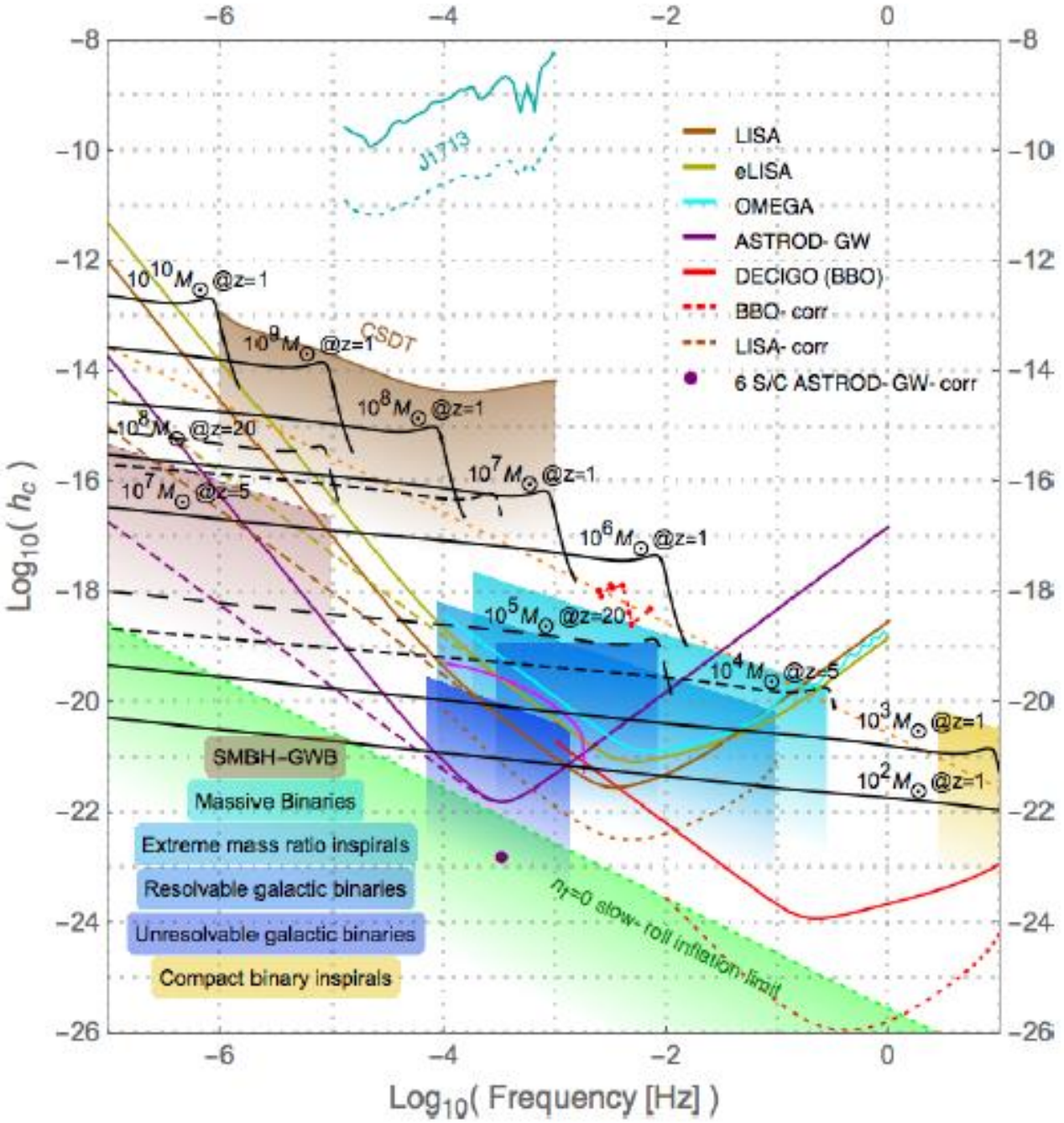
LISA
eLISA
OMEGA
ASTROD- GW
DECIGO (BBO)
BBO- corr
LISA- corr
6 S/C ASTROD- GW- corr
J1713
CSDT
$10^{10}M_\odot$@z=1
$10^{9}M_\odot$@z=1
$10^{8}M_\odot$@z=1
$10^{8}M_\odot$@z=20
$10^{7}M_\odot$@z=1
$10^{7}M_\odot$@z=5
$10^{6}M_\odot$@z=1
$10^{5}M_\odot$@z=20
$10^{4}M_\odot$@z=5
$10^{3}M_\odot$@z=1
$10^{2}M_\odot$@z=1
SMBH-GWB
Massive Binaries
Extreme mass ratio inspirals
Resolvable galactic binaries
Unresolvable galactic binaries
Compact binary inspirals
n_t=0 slow- roll inflation limit
$\mathrm{Log}_{10}(h_c)$
Log_{10}(Frequency [Hz])

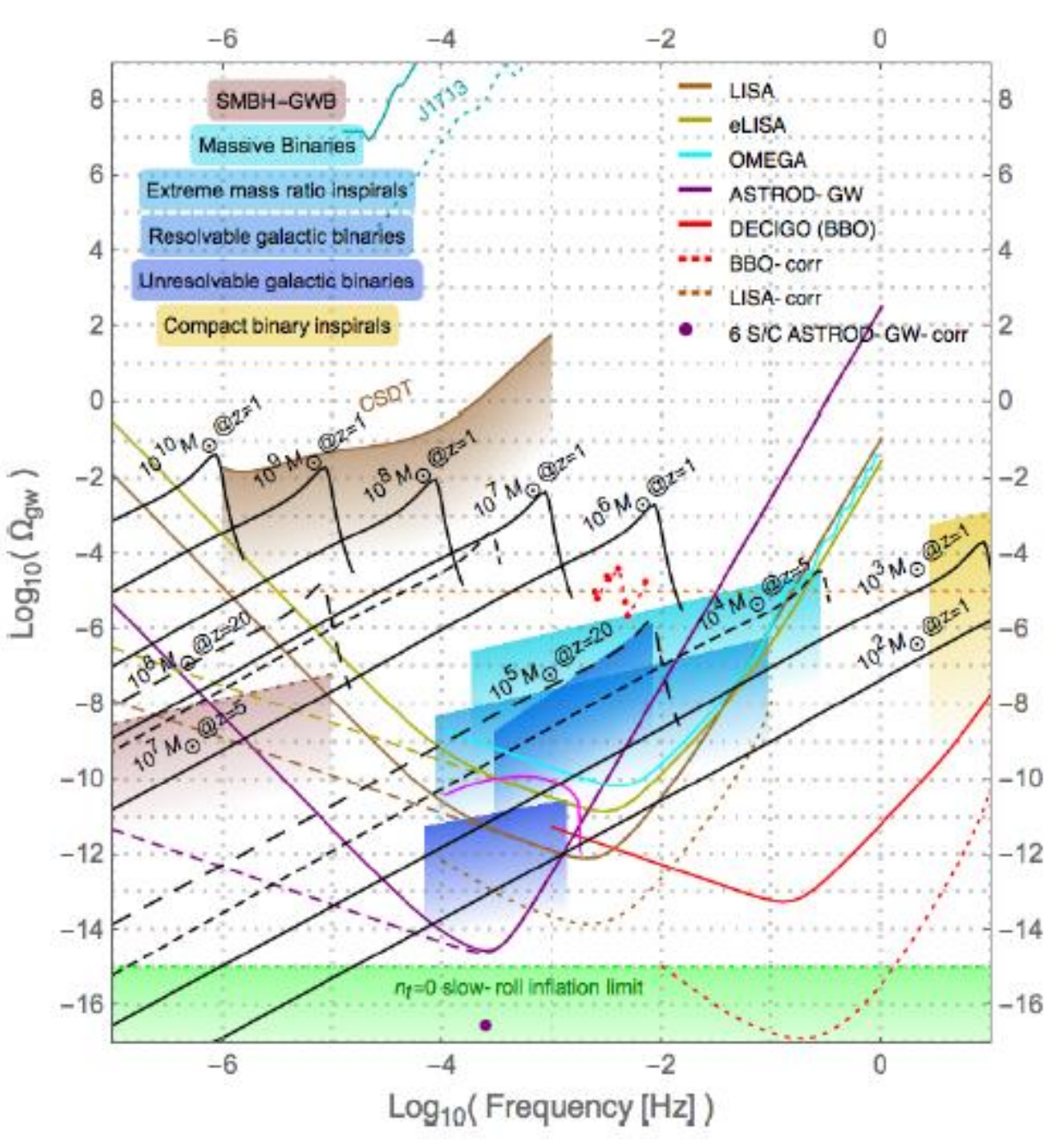
SMBH-GWB
Massive Binaries
Extreme mass ratio inspirals
Resolvable galactic binaries
Unresolvable galactic binaries
Compact binary inspirals
LISA
eLISA
OMEGA
ASTROD- GW
DECIGO (BBO)
BBO- corr
LISA- corr
6 S/C ASTROD- GW- corr
J1713
CSDT
$10^{10}M_\odot$@z=1
$10^{9}M_\odot$@z=1
$10^{8}M_\odot$@z=1
$10^{8}M_\odot$@z=20
$10^{7}M_\odot$@z=1
$10^{7}M_\odot$@z=5
$10^{6}M_\odot$@z=1
$10^{5}M_\odot$@z=20
$10^{4}M_\odot$@z=5
$10^{3}M_\odot$@z=1
$10^{2}M_\odot$@z=1
n_t=0 slow- roll inflation limit
$\mathrm{Log}_{10}(\Omega_{gw})$
Log_{10}(Frequency [Hz])

Conversion factors among:
the characteristic strain $h_c(f)$,
the strain psd (power spectral density) $[S_h(f)]^{1/2}$
the normalized spectral energy density $\Omega_{gw}(f)$

- $h_c(f) = f^{1/2}\,[S_h(f)]^{1/2}$;
- *normalized GW spectral energy density* $\Omega_g(f)$: GW spectral energy density in terms of *the energy density per logarithmic frequency interval divided by the cosmic closure density* ρ_c for a cosmic GW sources or background, i.e.,
- $\Omega_{gw}(f) = (f/\rho_c)\,d\rho(f)/df$
- $\Omega_{gw}(f) = (2\pi^2/3H_0^2)\,f^3\,S_h(f) = (2\pi^2/3H_0^2)\,f^2\,h_c^2(f)$.

	Characteristic strain $h_c(f)$	Strain psd $[S_h(f)]^{1/2}$	Normalized spectral energy density $\Omega_{gw}(f)$
$h_c(f)$	$h_c(f)$	$f^{1/2}\,[S_h(f)]^{1/2}$	$[(3H_0^2/2\pi^2f^2)\Omega_{gw}(f)]^{1/2}$
Strain psd $[S_h(f)]^{1/2}$	$f^{-1/2}h_c(f)$	$[S_h(f)]^{1/2}$	$[(3H_0^2/2\pi^2f^3)\Omega_{gw}(f)]^{1/2}$
$\Omega_{gw}(f)$	$(2\pi^2/3H_0^2)\,f^2\,h_c^2(f)$	$(2\pi^2/3H_0^2)\,f^3\,S_h(f)$	$\Omega_{gw}(f)$

Strain power spectral density (psd) amplitude vs. frequency for various GW detectors and GW sources

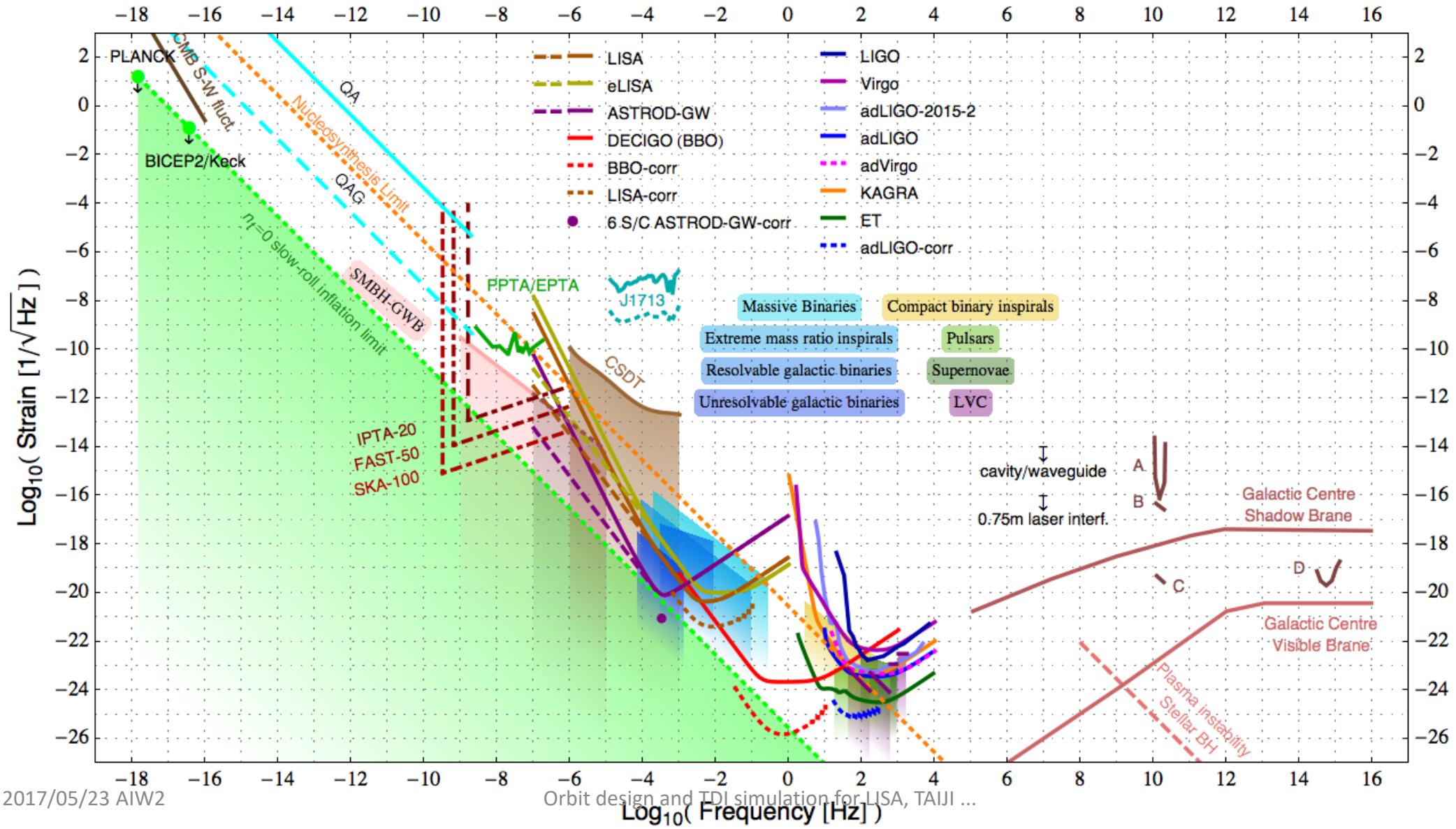

Characteristic strain h_c vs. frequency for various GW detectors and sources. [QA: Quasar Astrometry; QAG: Quasar Astrometry Goal; LVC: LIGO-Virgo Constraints; CSDT: Cassini Spacecraft Doppler Tracking; SMBH-GWB: Supermassive Black Hole-GW Background.]

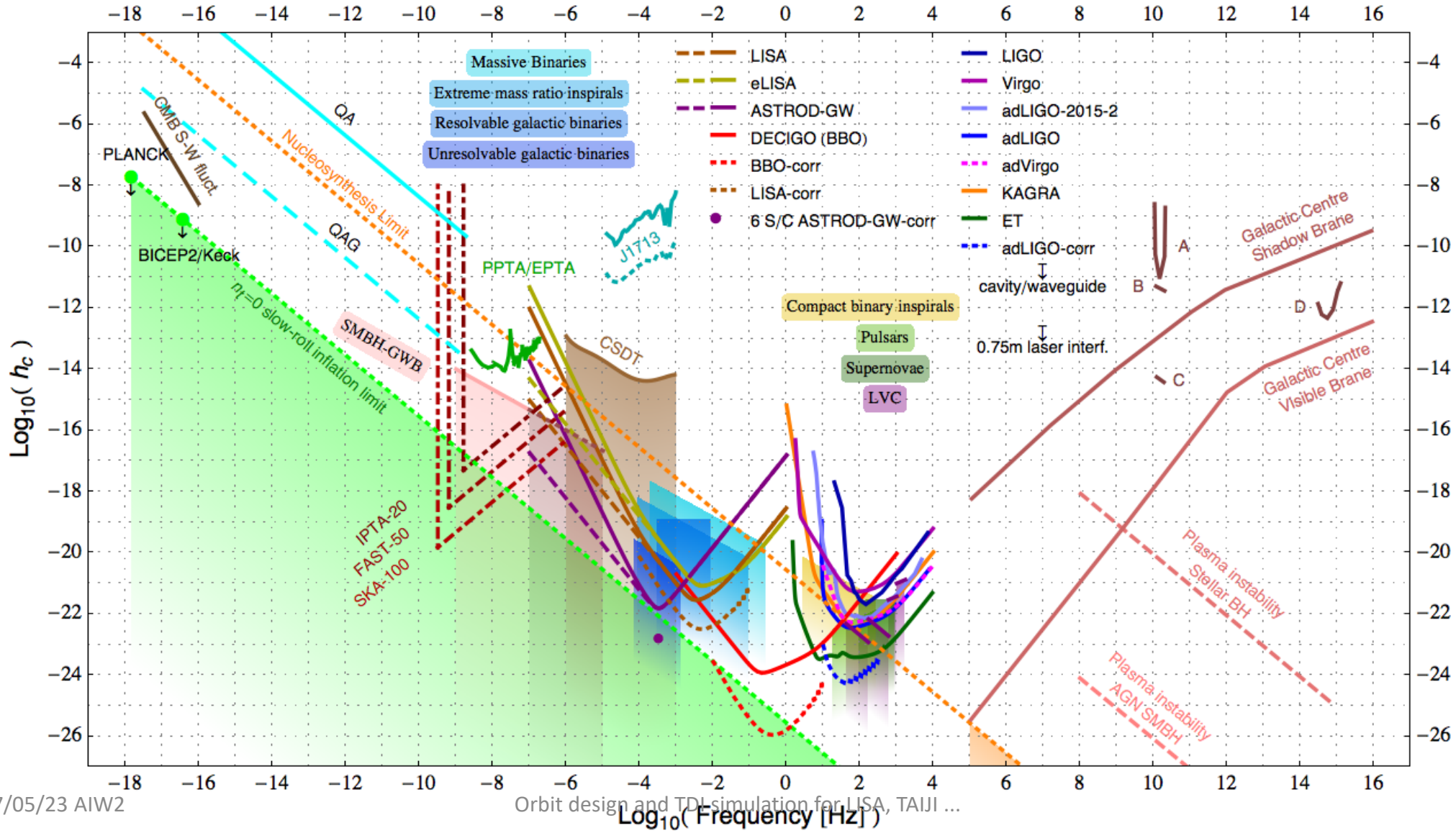

Normalized GW spectral energy density Ω_{gw} vs. frequency for GW detector sensitivities and GW sources

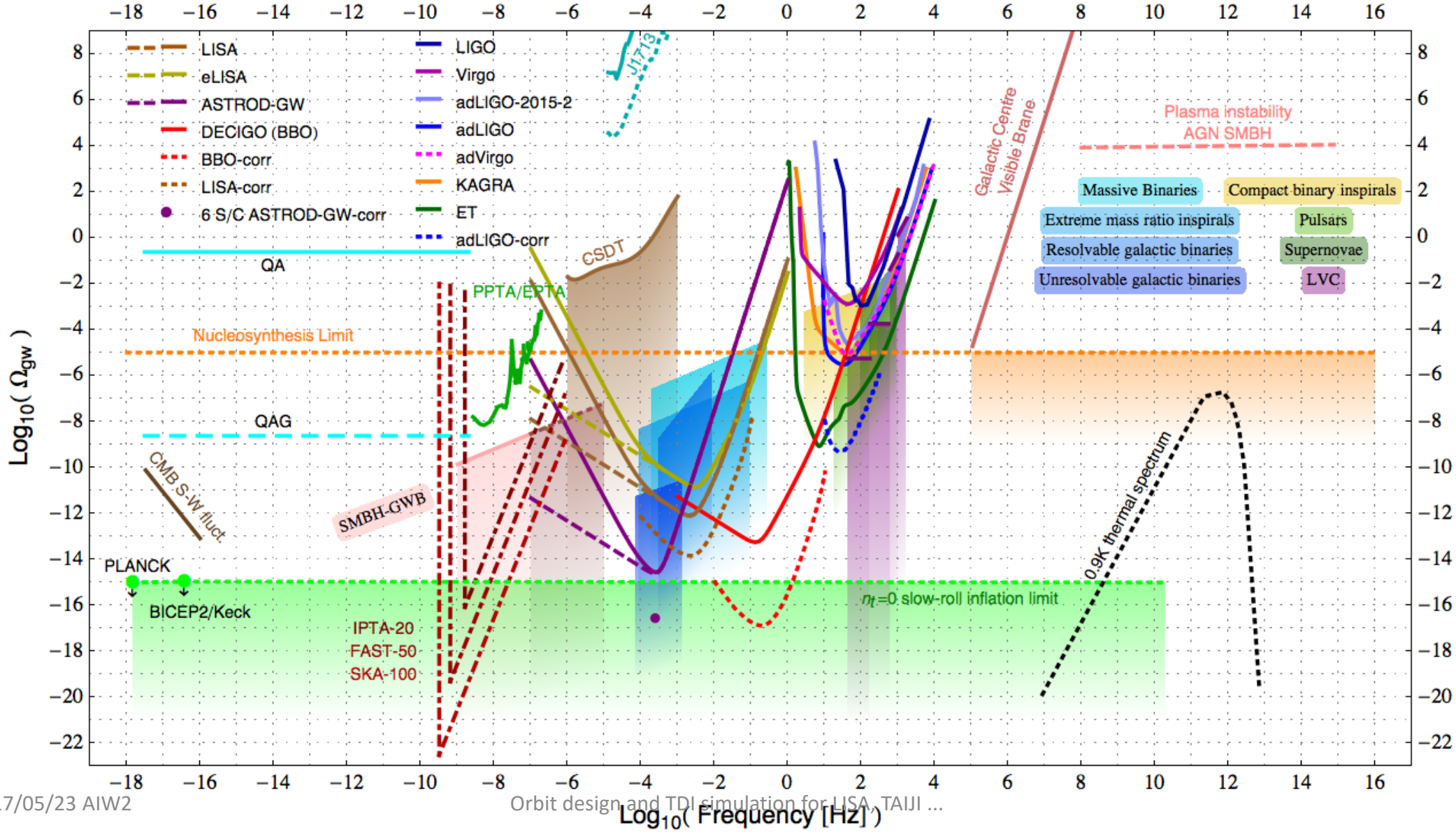

Detection Methods other than Laser Interferometry for Low-frequency and Middle-frequency GWs

- Radio-wave Doppler frequency tracking
- Atom Interferometry involving repeatedly imprinting the [hase of optical field onto the motional degrees of freedom of the atoms using light propagating back and forth between the spacecraft.
- Resonant Atom Interferometry detection
- GW detection with optical lattice atomic clocks


Thank
You